Journal Pre-proof

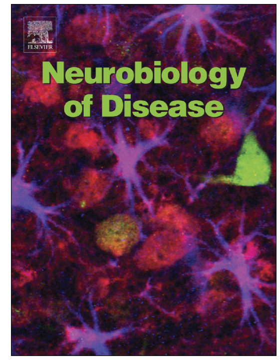

Impaired dopamine- and adenosine-mediated signaling and plasticity in a novel rodent model for DYT25 dystonia

Libo Yu-Taeger, Thomas Ott, Paola Bonsi, Celina Tomczak, Zinah Wassouf, Giuseppina Martella, Giuseppe Sciamanna, Paola Imbriani, Giulia Ponterio, Annalisa Tassone, Julia M. Schulze-Hentrich, Rose Goodchild, Olaf Riess, Antonio Pisani, Kathrin Grundmann-Hauser, Huu Phuc Nguyen

PII: S0969-9961(19)30309-2

DOI: https://doi.org/10.1016/j.nbd.2019.104634

Reference: YNBDI 104634

To appear in: *Neurobiology of Disease*

Received date: 25 July 2019

Revised date: 19 September 2019

Accepted date: 2 October 2019

Please cite this article as: L. Yu-Taeger, T. Ott, P. Bonsi, et al., Impaired dopamine- and adenosine-mediated signaling and plasticity in a novel rodent model for DYT25 dystonia, *Neurobiology of Disease*(2018), https://doi.org/10.1016/j.nbd.2019.104634

Impaired dopamine- and adenosine-mediated signaling and plasticity in a novel rodent model for DYT25 Dystonia

Libo Yu-Taeger[1,2], Thomas Ott[1,7], Paola Bonsi[3], Celina Tomczak[1,2], Zinah Wassouf[1,2], Giuseppina Martella[3,4], Giuseppe Sciamanna[3,4], Paola Imbriani[3,4] ,Giulia Ponterio[3,4,] Annalisa Tassone[3,4], Julia M Schulze-Hentrich[1,2], Rose Goodchild[5], Olaf Riess[1,2], Antonio Pisani[3,4], Kathrin Grundmann-Hauser[1,2,1], Huu Phuc Nguyen[1,6,1,*]
huu.nguyen-r7w@rub.de

[1]Institute of Medical Genetics and Applied Genomics, University of Tuebingen, Tuebingen, Germany

[2]Centre for Rare Diseases (ZSE), University of Tuebingen, Tuebingen, Germany

[3]Laboratory of Neurophysiology and Plasticity, IRCCS Fondazione Santa Lucia, Rome, Italy

[4]Department of Systems Medicine, University of Rome "Tor Vergata," Rome, Italy

[5]Center for the Biology of Disease/ Laboratory of Dystonia Research, Catholic University of Leuven, Leuven, Belgium

[6]Department of Human Genetics, Faculty of Medicine, Ruhr University Bochum, Bochum, Germany

[7]Core Facility Transgenic Animals, University Clinics Tuebingen, Tuebingen, Germany

*Corresponding author at: Department of Human Genetics, Ruhr University Bochum, Universitaetsstrasse 150, 44801 Bochum.

Abstract

Dystonia is a neurological movement disorder characterized by sustained or intermittent involuntary muscle contractions. Loss-of-function mutations in the *GNAL* gene have been identified to be the cause of “isolated” dystonia DYT25. The *GNAL* gene encodes for the guanine nucleotide-binding protein G(olf) subunit alpha ($G\alpha_{olf}$), which is mainly expressed in the olfactory bulb and the striatum and functions as a modulator during neurotransmission coupling with D1R and A2AR. Previously, heterozygous $G\alpha_{olf}$ -deficient mice (*Gnal*$^{+/-}$) have been generated and showed a mild phenotype at basal condition. In contrast, homozygous deletion of *Gnal* in mice

[1] equal contribution

(*Gnal*$^{-/-}$) resulted in a significantly reduced survival rate. In this study, using the CRISPR-Cas9 system we generated and characterized heterozygous *Gnal* knockout rats (*Gnal*$^{+/-}$) with a 13 base pair deletion in the first exon of the rat *Gnal* splicing variant 2, a major isoform in both human and rat striatum. *Gnal*$^{+/-}$ rats showed early-onset phenotypes associated with impaired dopamine transmission, including reduction in locomotor activity, deficits in rotarod performance and an abnormal motor skill learning ability. At cellular and molecular level, we found down-regulated *Arc* expression, increased cell surface distribution of AMPA receptors, and the loss of D2R-dependent corticostriatal long-term depression (LTD) in *Gnal*$^{+/-}$ rats. Based on the evidence that D2R activity is normally inhibited by adenosine A2ARs, co-localized on the same population of striatal neurons, we show that blockade of A2ARs restores physiological LTD. This animal model may be a valuable tool for investigating $G\alpha_{olf}$ function and finding a suitable treatment for dystonia associated with deficient dopamine transmission.

Keywords: GNAL, knockout, rat model, dopamine signalling, adenosine signalling, locomotor activity, LTD, *Arc*, AMPA receptor

Introduction

Dystonia is a neurological movement disorder characterized by sustained or intermittent involuntary muscle contractions causing abnormal, often repetitive, movement, posture, or both (Albanese *et al.*, 2013). Based on their first appearance in the literature, 26 types of primary (isolated) dystonia have been identified according to clinical and genetic features (Klein, 2014). Dystonia type 25 (DYT25) is an autosomal dominant inherited form caused by mutations in the *GNAL* gene including nonsense, missense, in-frame deletion and frameshift mutation (Fuchs *et al.*, 2013; Vemula *et al.*, 2013a; Kumar *et al.*, 2014; Masuho *et al.*, 2016).

The *GNAL* gene locus at chromosome 18p11, encodes for the guanine nucleotide-binding protein G(olf) subunit alpha ($G\alpha_{olf}$), an isoform of $G\alpha s$. $G\alpha_{olf}$ and $G\alpha s$ share extensive amino acid identity (80% in mice and 88% in rats) (Masters, Stroud and Bourne, 1986; Jones and Reed, 1989), but exhibit distinct expression patterns in the brain. $G\alpha_{olf}$ is predominant in the olfactory bulb and striatum, while $G\alpha s$ is expressed in the other brain regions (Hervé *et al.*, 1993; Hervé, Rogard and Lévi-Strauss, 1995;

Belluscio *et al.*, 1998; Kull, Svenningsson and Fredholm, 2000). Similar to Gαs, Gα_{olf} functions as a signaling G-protein coupled with both D1 dopamine receptor (D1R) and adenosine A2A receptor (A2AR) expressed on spiny projection neurons (SPNs) of the direct and the indirect striatal output pathway, respectively (Zhuang, Belluscio and Hen, 2000; Hervé *et al.*, 2001; Schwindinger *et al.*, 2010). After the receptor-ligand binding, G-protein promotes the conversion of ATP to cAMP via adenylyl cyclase (AC), and further activates the cAMP/PKA-signaling, controlling gene expression and synaptic plasticity (Cole *et al.*, 1992; Berke *et al.*, 1998; Zhang *et al.*, 2002; Jayanthi *et al.*, 2009). Accordingly, *GNAL* mutations result in a loss of function of Gα_{olf} leading to an impaired signal transduction of the D1R- or A2AR-mediated signaling pathway (Kebabian, Petzold and Greengard, 1972, 1972; Hervé *et al.*, 1993; Zhuang, Belluscio and Hen, 2000). Corticostriatal plasticity represents a well-established experimental paradigm of motor learning and memory, and is critically dependent on dopamine receptor-mediated transmission (Pisani *et al.*, 2005). Although traditional models of basal ganglia circuitry predict a schematic competition between direct and indirect pathways, there is emerging functional evidence for coordinated activation of both SPNs pathways during motor behavior, suggesting that *GNAL* mutations would likely affect both pathways (Bagetta *et al.*, 2011; Cui *et al.*, 2013; Goodchild, Grundmann and Pisani, 2013)**.** However, the precise cellular and molecular mechanisms underlying neuronal functional abnormalities and altered motor behavior in DYT25 remain unclear.

Human *GNAL* has 5 protein coding isoforms (http://www.ensembl.org/Homo_sapiens/Gene/Summary?g=ENSG00000141404;r=18:11688956-11885685), while rat (http://www.ensembl.org/Rattus_norvegicus/Gene/Summary?db=core;g=ENSRNOG00000010440;r=18:62805410-62944630) and mouse (http://www.ensembl.org/Mus_musculus/Gene/Summary?g=ENSMUSG00000024524;r=18:67088336-67226792) *Gnal* has 3 and 2 isoforms, respectively. According to databases (Ensembl and UniProt database), human (NM001142339), rat (G3V8E8) and mouse (NM010307) isoform 2 are orthologous with 98% identity. Human DYT25 is mostly caused by heterozygous mutations in *GNAL* isoform 2 or isoforms including isoform 2 (Fuchs *et al.*, 2013; Vemula *et al.*, 2013b; Kumar *et al.*, 2014; Masuho *et al.*, 2016), with the exception of one case caused by a homozygous c.1216C>T(p.R329W) missense mutation in *GNAL* isoform 1 (NM182978) leading to childhood-onset generalized dystonia, whereas heterozygous relatives did not display any overt dystonia (Masuho *et al.*, 2016). It has been ascertained that human *GNAL* isoform 2 is the major isoform since it showed an approximate 10 fold higher mRNA expression compared to isoform 1 in the human striatum, while other isoforms were not detectable (Vemula *et al.*, 2013a). Altogether, this indicates an important role of *GNAL* isoform 2 in both physiological and pathological conditions in DYT25.

Previously, a mouse *Gnal* knockout model was generated by the replacement of the first 4 exons with a pgk-neo cassette resulting in a null mutation in the $G\alpha_{olf}$ protein encompassing all isoforms (Belluscio *et al.*, 1998). These mice displayed dystonia-like movement, when they were challenged with DR1 agonist or compounds elevating extracellular dopamine in the striatum. However, they showed only mild phenotypes at basal condition, which are related to impaired D1R signaling (Belluscio *et al.*, 1998; Corvol *et al.*, 2001, 2007; Pelosi *et al.*, 2017).

In the present study, we generated a rat model for DYT25 to provide a second animal model of a different species and analyze disease expression under the condition of genetically knocking out the major isoform of *Gnal* (G3V8E8) only. Investigations in the behavioral, electrophysiological and biochemical domains in $Gnal^{+/-}$ rats at basal condition demonstrated early-onset pathological motor phenotypes, which are related to altered $G\alpha_{olf}$-dependent signaling pathways.

Material and methods

Animals

All rats used on the Sprague-Dawley background (Crl:CD(SD)) were housed with littermates of mixed genotype in groups of 3-4 on a 12 h light/dark cycle with free access to food and water.

The generation of the loss of-function allele was performed using the CRISPR/Cas9 technology. Putative guide RNA sequences targeting the first exon of the rat *Gnal* gene isoform 2 were designed with the help of various online tool kits. Oligonucleotides containing a putative guide RNA sequence (5´gaccgcggaagatcagggcg3´) were cloned into the px330-vector (Addgene). Preparation and purification of guide RNA and Cas9 mRNA were performed as described before (Cong *et al.*, 2013; Harms *et al.*, 2014; Kaneko, 2017).

All components were injected into the pronucleus of rat zygotes with various concentrations.

All experiments were approved by the local ethics committee at Regierungspraesidium Tuebingen (License Number: HG1/14), and carried out in accordance with the German Animal Welfare Act and the guidelines of the Federation of European Laboratory Animal Science Associations, based on European Union legislation (Directive 2010/63/EU). The experiments described in the Electrophysiology section were approved by the ethics committees of IRCCS Fondazione Santa Lucia and of University of Rome Tor Vergata, and authorized by the Italian Ministry of Health (authorization nr. 223-2017-PR). These procedures were conducted in accordance with the Italian law (D.Lgs 26/2014), and the European Union Directive 2010/63/EU.

For behavioural experiments, same cohorts of male rats were used, n=10 and n=9 for *Gnal*$^{+/-}$ rats and for WT littermates respectively.

Rotarod test

Male *Gnal*$^{+/-}$ rats and WT littermates were tested every month between 3 and 9 months of age. Rats were trained at a constant speed of 12 rpm/min before the actual tests, as they received 12 training sessions in 3 consecutive days at the 1st testing point (3 months) and 4 training sessions in one day in the following months. Each training session lasted 2 minutes, rats were returned back to the rod after falling during one session. Two tests were performed directly after the training days within one day at an accelerated speed from 4 to 40 rpm over a period of 4 min, and then operated constantly at 40 rpm for the last min. The latency to fall was recorded and the mean of two tests was taken for the analysis. If the rat did not fall within 5 min, the test would be ended and recorded as 5 min.

Locomotor movement assessment

To assess the locomotor activity, rats were monitored using the PhenoMaster system (TSE Systems), which represents a modular setup that screens rats in a home cage-like environment for their ambulatory activity and rearing as well as feeding and drinking behavior. The activity detection is achieved using infrared sensors arranged in horizontal (x,y) level for ambulatory activity and vertical (z) level for rearing. The number of beam breaks represents locomotor movements and the repeated beam break of the same light barrier is defined as fine movement. The same cohort of male rats was monitored for 22 h every 3 months until 12 months of age. Data were automatically collected with 20 min intervals and analyzed either for the dark (active) phase only or for the whole light cycle (total).

Primary cell culture and treatment

E18 primary striatal neurons were prepared by an adapted method based on a previously described protocol (Friedman *et al.*, 1993). After the dissection in dissection buffer (0.7 g HEPES, 0.168 g NaHCO3, 200ml calcium-magnesium-free (-/-) HBSS medium (Lifetechnology, Gibo)), striata were minced into approximately 1 mm^3 pieces and washed in (-/-) HBSS medium containing 2% B-27 (Lifetechnology, Gibo). Following the incubation in digestion solution (40 µl 0.25% Trypsin in 0.5 ml calcium-magnesium-containing (+/+) HBSS medium (Lifetechnology, Gibo)) for 15 min at 37°C, the tissues were triturated with a fire polished Pasteur pipette in triturating solution ((+/+) HBSS medium, 4% BSA (Thermo Fisher Technology), 5mg/ml DNase I (Sigma), 2% B-27) and centrifuged for 5 min at 250 rcf to dissociate and harvest neuronal cells. Primary striatal neurons were seeded onto Poly-D-Lysine coated coverslips in 24-well plates at a density of 50,000 cells/cm^2 for the immunostaining and into 6-well plate at a density of 1.0 x 10^6 cells/well for the biochemistry analyses in neuronal growth media (2% B-27, 0.5mM glutamine (Sigma), Neurobasal (Lifetechnology, Gibo). The cells were incubated at 37°C and supplied with 5% CO2 in a humidified incubator. Every 3/4 days, half of the media were exchanged for fresh neuronal growth media. Before cells were harvested for the immunocytochemistry analysis and surface protein assay, one group of cells was treated with 0.1 µM SKF83822 (Tocris Bioscience) a D1R agonist in growth media for 20 minutes at room temperature.

Surface protein assay

Surface α-amino-3-hydroxy-5-methyl-4-isoxaazoleoropionic acid receptor (AMPAR) was labeled with sulfo-NHS biotin and isolated using a cell surface protein isolation kit (Pierce, 89881, ThermoFisher Sceintific) following manufacturer's instruction. For each sample 4 million cells were used, and lysed, following incubation in sulfo-NHS biotin and wash steps. After the centrifugation of cell lysate 30 µl supernatant of each sample was collected as total protein control, the rest was passed through the NeutrAvidin agarose column to isolate biotin-labeled surface protein. AMPARs were detected in surface and total protein fraction using Western blot. SCN4B sodium channel beta4 subunit was used as loading reference for the surface protein fraction, while GAPDH was used as the reference for the whole protein fraction.

Protein extraction from tissue

The protein expression level of Activity-regulated cytoskeleton-associated protein (ARC) was compared between *Gnal*$^{+/-}$ rats und WT littermates using Western blotting. Striatal tissue was obtained from rats at 3 and 12 months of age (n=6 for each group at each time point), after dissection tissue was snap frozen in liquid nitrogen and stored at -80 °C till use. For the protein extraction, striatal tissue was homogenized with a homogenizer type T25 (Janke und Kunkel GmbH) at a speed of 30,000 rpm in a modified RIPA buffer (150 mM sodium chloride, 1.0% NP-40, 0.5% sodium deoxycholate, 0.1% SDS, 50 mMTris, 5 mM EDTA pH8.0) supplemented with proteinase inhibitor cocktail complete without EDTA (Roche Diagnostics) and phosphatase inhibitor PhosSTOP (Sigma).

Immunoblotting

For the Western blot analyses, equal amounts of protein of each sample were separated on 4-12% NovexNuPAGE Bis-Tris gels (Invitrogen Life Technologies). Membranes were incubated overnight at 4°C in primary antibodies: anti-Gα_{olf} at a dilution of 1:1000 (ThermoFisher Scientific, PA5-27964), anti-ARC at a dilution of 1: 750 (Synaptic Systems, 156003), anti-AMPAR at a dilution of 1:500 (Cell signaling, 13185), anti-pERK at a dilution of 1:750 (Cell signaling, 4376), and anti-ERK at a dilution of 1:300 (Santa Cruz, sc-27120). Secondary antibodies coupled with either florescence or HRP were incubated for 2 hours at room temperature. Protein bands were visualized and analyzed with Odyssey Imaging System and the software Images Studio (Licor Sciences).

Quantification of gene expression level

Male rats at 3 and 12 months of age were sacrificed by CO_2 asphyxiation, brains were quickly removed and striata were dissected on ice. Striatal tissues were stored at -80°C after snap-freezing in liquid nitrogen. Total RNA extraction was performed using RNeasy Plus Mini Kit (Qiagen) following manufacturer's instruction. 100 ng of total RNA was used for the reverse transcription reaction (QuantiTect Reverse Transcription kit, Qiagen). The resulting cDNA was diluted (1:20) and 2 µl were then used for the qPCR assay, mixed with primers (0.5 µM) and SYBR green master mix (Qiagen). Each primer sequence was summarized in supplementary table 1(S1). Relative expression was calculated based on Pfaffl model (Pfaffl, 2001) after normalization to the geometric mean relative expression of two reference genes (Eif4a2 and Gapdh), which were previously assessed for their stable expression using Normfinder (Andersen, Jensen and Ørntoft, 2004) and Genorm (Vandesompele *et al.*, 2002). Data were calculated using Excel-based equations.

Immunohistological staining

For the immunohistological staining, brains of male rats at 3 and 12 months of age were fixed by transcardiac perfusion with 4% paraformaldehyde (PFA) in PBS, followed by post-fixation with the same fixatives overnight at 4 °C. After cryoprotection in 30% sucrose/PBS solution, 40 µm coronal brain cryosections were cut serially at 240 µm intervals, every 6th striatal brain section was chosen for the analyses of $G\alpha_{olf}$ expression in an anatomical context. Free-floating staining was performed as previously described (Yu-Taeger *et al.*, 2012), the whole procedure was carried out at room temperature. The endogenous peroxidase activity of brain sections was blocked by using 0.5% sodium borohydride, followed by section permeabilization in TBS containing 0.4% Triton X-100 (TBST). The incubation in primary antibody anti-$G\alpha_{olf}$ (ThermoFisher Scientific, PA5-27964) was performed overnight at a dilution of 1:1000, followed by secondary antibody staining using biotinylated goat anti-rabbit at a dilution of 1:1000 (Vector Laboratories). Then sections were treated with an avidin–biotin complex (Vector Laboratories, BA-1000), and exposed to DAB-H_2O_2 (0.01% DAB, and 0.001% hydrogen peroxide) until a suitable staining intensity had developed.

Immunocytochemistry and data analysis

Striatal neurons at DIV21 were fixed with 4% paraformaldehyde /0.1 M PBS solution containing 4% sucrose for 10 min at room temperature. Following the blocking step in 10% normal goat serum, cells were incubated with anti-AMPAR at a dilution of 1:200 overnight at 4°C (Cell signaling, 13185). Immunofluorescence conjugated secondary antibody was used at a dilution of 1:500. The whole staining process was carried out in PBS without permeabilization reagent.

Quantification of surface AMPAR puncta was carried out using ImageJ (NIH), as previously described (Rumbaugh *et al.*, 2003; Shepherd *et al.*, 2006). Images were thresholded at a cluster *p* value of 0.05. The same length of dendrite segments (50 µm) was selected at approximately 10 µm distance from dendrite origin for each neuron. Pixel area and total fluorescence intensity were compared between *Gnal*$^{+/-}$ and *Gnal*$^{+/+}$ neurons (n=30 per group).

Electrophysiology

Tissue slice preparation: Rats were sacrificed by decapitation under halothane anesthesia, the brains were immediately removed from the skulls and cut with a vibratome (Leica Microsystems) in Krebs' solution (in mM: NaCl (126), KCl (2.5), MgCl2 (1.3), NaH2PO4 (1.2), CaCl2 (2.4), glucose (10), NaHCO3 (18)), bubbled with 95% O2 and 5% CO2. Coronal and parasagittal corticostriatal slices (200 µm thick for patch-clamp recordings, 300 µm for sharp-electrode recordings) recovered in oxygenated Krebs' solution for about 30-60 minutes, and then were transferred into a recording chamber, continuously superfused with oxygenated Krebs' solution, and maintained at 32 - 33 °C.

Electrophysiological recordings: Recordings were made with either Axoclamp 2B (sharp-electrode recordings) or AxoPatch 200B and Multiclamp 700B (patch-clamp recordings) amplifiers, coupled to pClamp 10software (Molecular Devices). Borosilicate glass pipettes (resistance 30 - 60 MΩ for intracellular recordings, and 2.5 - 5 MΩ for patch-clamp recordings) were pulled on P-97 pullers (Sutter Instruments). For patch-clamp recordings, neurons were visualized using differential interference contrast and infrared optics, and a monochrome CCD camera. For whole-cell recordings of spiny projection neurons (SPNs), electrodes were filled with an intracellular solution containing the following (in mM): K^+-gluconate (125), NaCl (10), CaCl2 (1.0), MgCl2 (2.0), 1,2bis (2-aminophenoxy)ethane-N,N,N,N-tetra-acetic acid

(BAPTA) (0.1), HEPES (10), GTP (0.3) Mg -ATP (2.0); pH 7.3. Membrane currents were continuously monitored and access resistance, measured in voltage-clamp, was within the 5 - 30 MΩ range. Basic electrophysiological properties of SPNs, such as resting membrane potential (RMP), input resistance (IR), rheobase and current-voltage relationship, were evaluated in the current-clamp configuration. Synaptic properties of excitatory postsynaptic currents (EPSCs) were analyzed in the voltage-clamp configuration. Paired-pulse facilitation (PPF) was evaluated at -70 mV holding potential (HP) in picrotoxin (PTX) (50 μM), by delivering two stimuli at 50-500 ms interstimulus interval (ISI) and measuring the EPSC2/EPSC1 ratio. Sharp-electrode intracellular recordings of SPNs were performed in the current-clamp configuration, by using borosilicate electrodes filled with 2M KCl. A bipolar electrode was placed in the corpus callosum to evoke corticostriatal excitatory postsynaptic potentials (EPSPs), in the presence of PTX (50 μM). High-frequency supra-threshold stimulation (HFS, three trains 3 s at 100 Hz, 20 s apart) was delivered to induce long-term depression (LTD) (Martella et al., 2009). The amplitude of EPSPs was plotted over-time as percentage of the pre-HFS control EPSP. Drugs were purchased from Tocris Cookson and Sigma Aldrich.

Immunohistochemistry: To identify recorded neurons as SPNs, electrodes were loaded with biocytin (Maltese *et al.*, 2018)**.** Briefly, slices were fixed with 4% PFA in 0.12 M phosphate buffer and 30 μm thick sections were cut from each slice with a freezing microtome, then dehydrated with serial alcohol dilutions to improve antigen retrieval and reduce background (Maltese *et al.*, 2018)**.** The following antibodies were utilized: goat anti-DARPP-32 (1:500 AF6259, R&D system) and anti-goat Alexa 647 (Invitrogen). Images were acquired with a LSM700 Zeiss confocal laser scanning microscope.

Statistical analysis

Electrophysiology data were analyzed offline using Clampfit 10 (Molecular Devices), Prism 6 (GraphPad), and Orgin 2016 (Adalta) softwares. All data are presented as mean ± SEM for each condition. Two-way repeated measures ANOVA with *Tukey's* posthoc test and with *Bonferroni* post hoc test were performed for analyzing behavioural tests, and electrophysiological paired-pulse experiments, respectively; two-tailed unpaired or paired Student's *t*-tests were used for electrophysiological, biochemical and immunological analysis; non-parametric Mann Whitney test was utilized for non-Gaussian distributions. $P<0.05$ was considered statistically significant. Sample size was determined using a priori Power Analysis (Statistical Solutions, LLC, Power & Sample Size Calculator).

Results

Generation of *Gnal* knockout rats

Gnal knockout rats were generated by CRISPR-Cas9 technology. Exon1 of rat *Gnal* splicing variant 2 was targeted mediating a sequence specific guide RNA (5'-CACCGCGGAAGATCAGGGCG-3'). Using DNA obtained from the founder rat a PCR product flanking the targeted region was sequenced. A deletion of 13 base pairs that corresponded to position 34-46 downstream of the translation start point ATG of the *Gnal* splicing variant 2 was detected resulting in an early stop at position 150 and producing a truncated protein with 50 amino acids (Fig. 1A and 1B).

It has been described that only 5% of homozygous *Gnal* knockout mice could survive till maturity (Belluscio *et al.*, 1998). We therefore analyzed the genotype distribution in 5 litters of *Gnal* knockout rats (in total 47 pups), which were obtained from crossing heterozygous *Gnal* knockout rats with each other. We found no significant difference between the observed ratio of genotypes and the expected ratio according to Mendelian laws (Chi-Square=1.44, 1.10, 1.44 for homozygotes, heterozygotes and WT, $p>0.05$) in new born rats. However, after birth homozygous mutants exhibited a significantly reduced survival rate of 75% due to death during infancy. The surviving homozygotes had a life span comparable to heterozygous and WT littermates with approximately 25% reduction in body weight (Supplementary Fig. 1; log rank test, p=0<0.05).

We compared protein expression level of $G\alpha_{olf}$ in different brain regions in a male and a female WT Sprague-Dawley rat at 2 months of age using Western blot analyses. An antibody binding to a region within amino acids 122 and 381 of protein $G\alpha_{olf}$, which is supposed to recognize all isoforms, was used for immunoblotting. No difference of $G\alpha_{olf}$ expression was observed between male and female rats (data not shown). In line with previous reports on the anatomical gene expression pattern, the most abundant mRNA expression of *Gnal* was found in the olfactory bulb and in the striatum in rodents (Drinnan *et al.*, 1991; Belluscio *et al.*, 1998). Western blot analysis revealed a major band at the appropriate size of 42 kDa in the striatum and the olfactory bulb with strong intensity, which was absent in the *Gnal* homozygous knockout rats and showed reduced intensity in *Gnal* heterozygous knockout rats. A $G\alpha_{olf}$-immunopositive band was also found in the amygdala with a markedly reduced intensity compared to the striatum and olfactory bulb. No $G\alpha_{olf}$-specific band was observed in the cerebral cortex, cerebellum, hippocampus and the brain stem. Moreover, we quantified the protein expression level of $G\alpha_{olf}$ in the striatum of male *Gnal* rats at 3 months of age (n=3 per genotype). We found a 50% reduction of $G\alpha_{olf}$ expression in $Gnal^{+/-}$ rats compared to WT littermates, while no $G\alpha_{olf}$ immunoreactivity could be detected in the striatum of $Gnal^{-/-}$ rats (Student's *t*-test, $p<0.01$) (Fig. 1C and D).

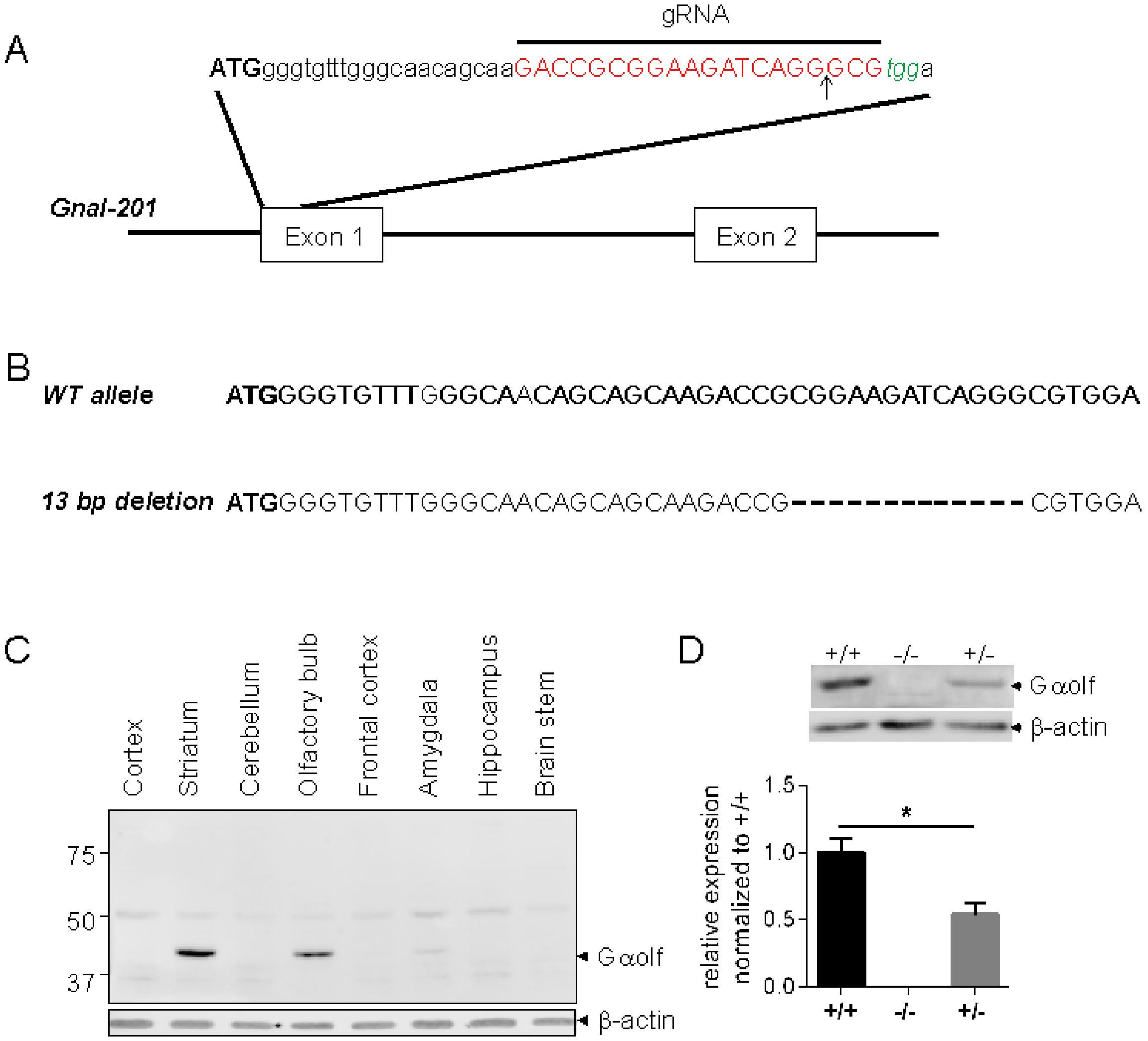

Figure 1. Generation of *Gnal* isoform 2 knock-out rats using CRISPR/Cas9. (A) Targeting the first exon of *Gnal* isoform 2. The sequence highlighted in green is the PAM

motif; the sequence in red capital letters is the sequence targeted by the small guide RNAs; the arrow indicates the Cas9 cutting site. (B) Sequences of the wild-type (WT) *Gnal* isoform 2 allele and of the targeted allele of *Gnal*$^{+/-}$ rats carrying 13 base pairs deletion. (C) Western blot analysis of $G\alpha_{olf}$ expression in various brain regions of adult WT Sprague-Dawley rat. (D) Quantitative analysis of protein expression level of $G\alpha_{olf}$ in the striatum of *Gnal*$^{+/-}$ rats at 3 months of age showed an approximately 50% reduction of $G\alpha_{olf}$ in *Gnal*$^{+/-}$ rats compared to WT littermates (n=3, Student's *t*-test). Striatal sample of a *Gnal*$^{-/-}$ rat served as negative control. Data are represented as mean ± SEM. *: $p<0.05$.

The reduction of $G\alpha_{olf}$ expression in *Gnal*$^{+/-}$ rats was confirmed using immunohistological staining. Coronal brain sections of *Gnal* knockout rats at 3 months and WT littermates were stained using anti-$G\alpha_{olf}$. In WT rats, the immunoreactivity of anti-$G\alpha_{olf}$ was observed in the epithelium layer of the olfactory bulb, but not in the glomerular layers, neither in the internal and external plexiform layers. The striatum showed $G\alpha_{olf}$ -immunoreactivity throughout the dorsal (caudate-putamen, CPu) and ventral area (nucleus accumbens, NAc). $G\alpha_{olf}$ -immunoreactivity was absent in *Gnal*$^{-/-}$ rats showing only background staining, while *Gnal*$^{+/-}$ rats displayed a reduced protein abundance in both the olfactory and the striatum compared to the WT control (Fig. 2).

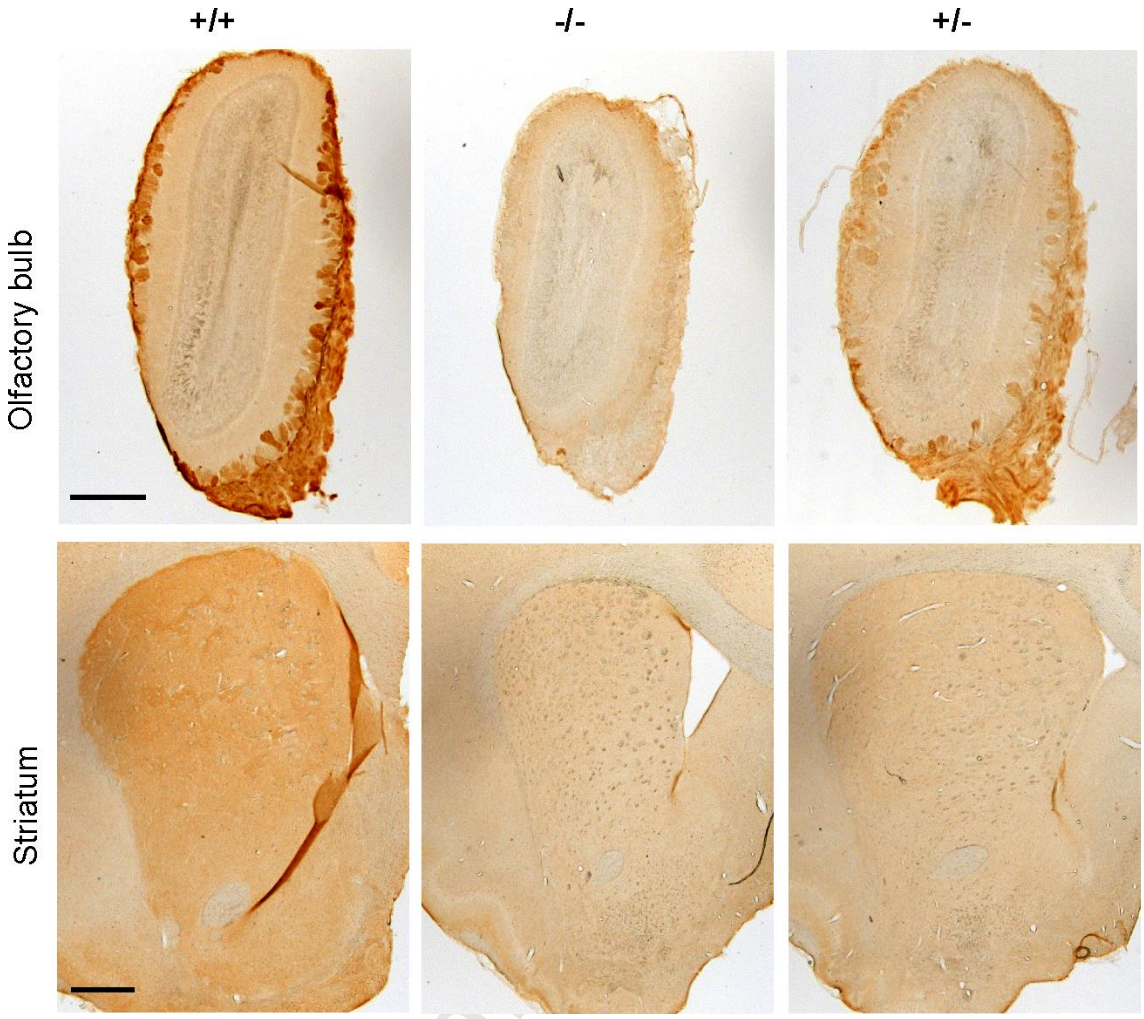

Figure 2. Immunohistochemical validation of Gα_{olf} expression in the olfactory bulb and striatum in *Gnal* knock-out rats at 3 months of age. Coronal brain sections of *Gnal*$^{+/+}$, *Gnal*$^{-/-}$ and *Gnal*$^{+/-}$ rats (n=3) were stained with anti-G$\alpha_{olf.}$ Representative images demonstrate the strong immunoreactivity of Gα_{olf} in the epithelium layer of olfactory bulb and throughout the striatum in WT rats, the signal intensity in those areas is markedly reduced in *Gnal*$^{+/-}$ rats while *Gnal*$^{-/-}$ rats only showed background staining. Scale bar: 1.0 mm.

Since most DTY25 patients carry a pathogenic *GNAL* mutation on only one allele, further phenotypic analysis of *Gnal* knockout rats were performed in heterozygous *Gnal*$^{+/-}$ rats.

Decreased locomotor activity in *Gnal*$^{+/-}$ rats

It is well known that locomotor activities depend on dopaminergic signaling (Beninger, 1983; Zhou and Palmiter, 1995), and that impaired signaling in the dopamine system causes hypoactivity in adult animals (Ungerstedt, 1979; Cortall and

Naylor, 1997). To investigate locomotor activity, the ambulatory activity and the rearing behavior of *Gnal*$^{+/-}$ rats and their WT littermates were measured in the PhenoMaster system. Male rats (n=10 for *Gnal*$^{+/-}$, n=9 for WT) were screened for 22 hours (12 h in the dark phase followed by 10 h in the light phase) every three months from 3 to 12 months of age. The ambulatory activity in rats of both genotypes decreased significantly with age from 3 to 12 months (age effect: $F(1,18)=107.8$ and 118.2 for dark phase and whole light/dark cycle, respectively, $p<0.0001$ for both). A significantly reduced ambulatory activity over the whole investigation period was demonstrated in *Gnal*$^{+/-}$ rats compared to WT animals in the active phase (dark phase) (Fig 3A) (genotype effect: $F(1, 18)=7.811$; $p<0.05$), as well as in a whole light/dark cycle (22h, Fig 3B) (genotype effect: ($F(1,18)=8.673$, $p<0.05$). The rearing behavior of *Gnal*$^{+/-}$ KO rats showed a trend towards a reduction. However, this did not reach statistical significance due to a high standard deviation (data not shown). For food intake and body weight we did not observe a significant difference between the genotypes at any time point (Fig. 3 C and 3D).

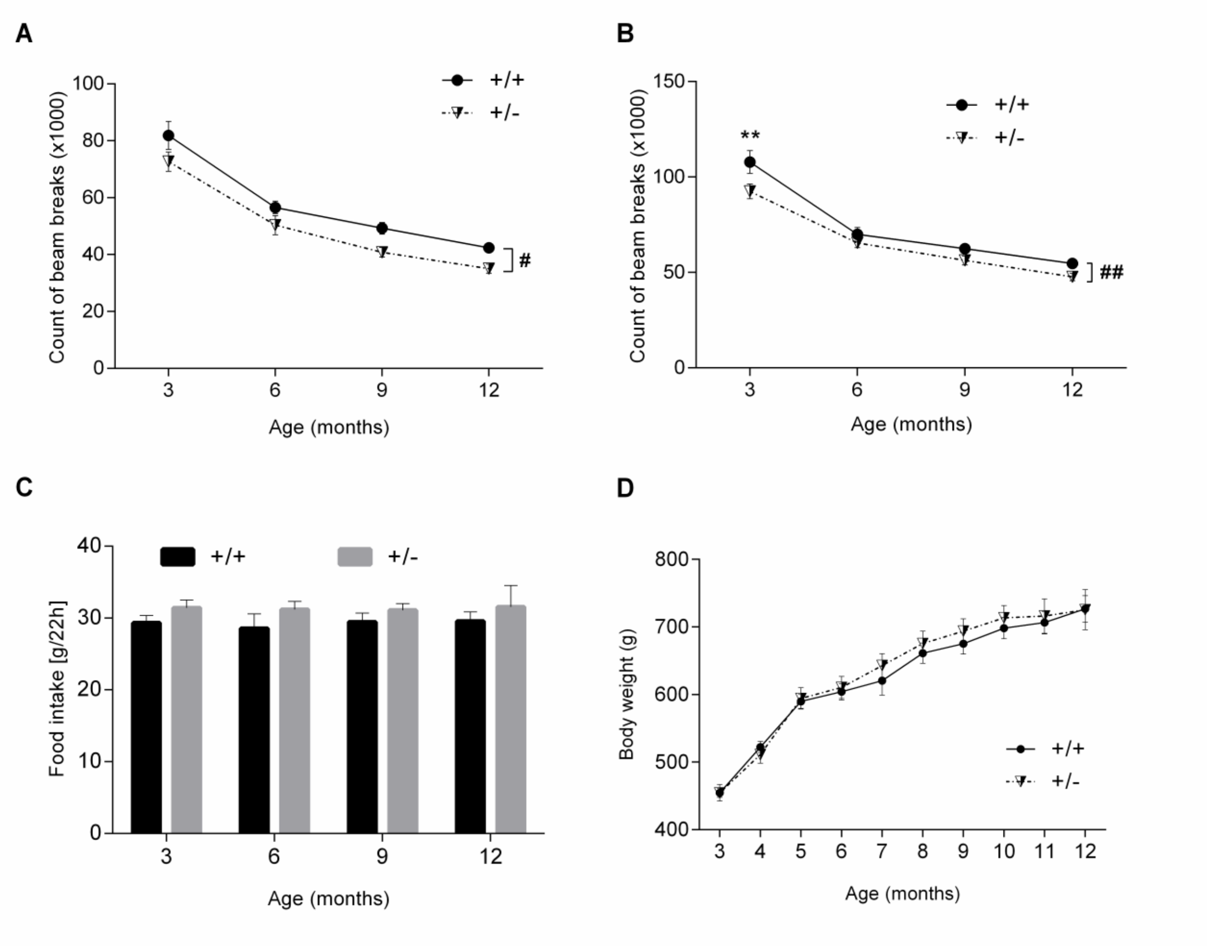

Figure 3. Reduced locomotor activity in *Gnal*$^{+/-}$ rats with normal food intake and body weight. Locomotor activity and food intake were monitored from 3 to 12 months of age every 3 months in the same cohort of rats (n=10 for *Gnal*$^{+/-}$ rats, n=9 for WT rats). Ambulatory activity was found significantly reduced in Gnal$^{+/-}$ rats over the whole investigated period in both dark phase (A) and whole light/dark cycle (B) (two-way repeated measures ANOVA with Tukey's post hoc test). No changes were found in food intake (C) and body weight (D). Data are represented as mean ± SEM. # indicates the results of two-way repeated measures ANOVA analysis; * indicates the results of Tukey's post hoc test. #: p<0.05; ##/**: *p*<0.01.

Impaired motor function and motor learning skills in *Gnal*$^{+/-}$ rats

Several animal models of dystonia exhibit, to different extent, deficits in motor coordination, often measured with the rotarod test, although overt dystonic movements and/or postures are not evident. Thus, an impairment at the rotarod test has been commonly utilized in dystonia (Oleas *et al.*, 2013). *Gnal*$^{+/-}$ rats and WT littermates were tested every month starting at 3 months of age. Two-way repeated measures ANOVA demonstrated a worse rotarod performance in *Gnal*$^{+/-}$ rats as they showed a significantly decreased latency to fall compared to WT littermates (genotype effect: $F(1,18)=7.587$, $p<0.01$). At 9 months of age, most *Gnal*$^{+/-}$ rats were unable to walk on the rod even at the lowest velocity (4 rpm), the test was therefore stopped at this time point. These results indicated an impaired motor function in *Gnal*$^{+/-}$ rats with an early age of onset (Fig. 4A). There was no progression of this motor deficit across the analyzed period in *Gnal*$^{+/-}$ rats, as no interaction between genotype and age was detected. One study utilizing the rotarod test has demonstrated that impaired dopamine signaling led to an altered motor skill learning (Shiotsuki *et al.*, 2010), similar results were observed in *Gnal*$^{+/-}$ mice (Pelosi *et al.*, 2017). Acquisition of motor skill learning was therefore evaluated by analyzing the number of falls during 12 training sessions on the rotarod at a constant speed (12 rpm). The rotarod performance of rats from both genotypes markedly increased during the first training day (first 4 training sessions) and reached a plateau until the last training day (9-12 training session). Two-way repeated measures ANOVA revealed a significant effect of genotype ($F(1,18)=6.161$, $p<0.05$). In particular, significant differences between the genotypes were present in session 2 and session 3 (Tukey's post hoc test, $p<0.01$ and $p<0.05$, Figure 4B). These results indicated impaired motor function and a motor skill learning deficit in *Gnal*$^{+/-}$ rats.

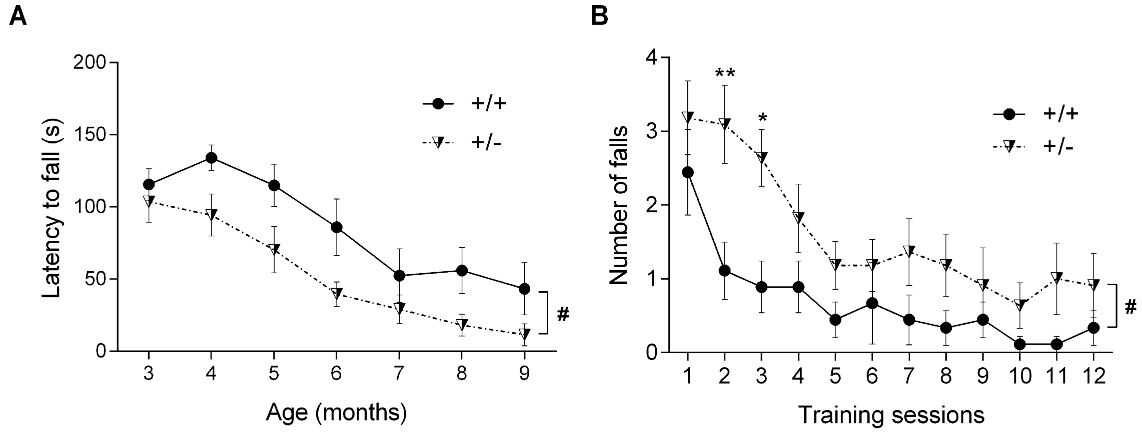

Figure 4. Motor deficit and impaired motor skill learning ability in *Gnal*$^{+/-}$ rats. Motor function and motor skill learning ability were analyzed by using the rotarod test. For the analysis of motor function rats underwent two test sessions each month from 3 to 9 months of age on an accelerated rod (4-40 rpm in 4 min) (n=10 for *Gnal*$^{+/-}$ rats, n=9 for WT rats). For the analysis of motor skill learning ability, the same cohort of rats was trained for 12 training sessions on 3 consecutive days at the first test point at 3 months of age. Latency to fall and number of falls were compared between *Gnal*$^{+/-}$ rats and WT littermates for the analysis of motor function and analysis of motor skill learning ability, respectively. Two-way repeated measures ANOVA analysis with *Tukey's* post hoc test revealed a poorer performance on the rotarod (A) and impaired motor skill learning ability in *Gnal*$^{+/-}$ rats. Data are represented as mean ± SEM. # indicates the results of two-way repeated measures ANOVA analysis; * indicates the results of Tukey's post hoc test. #/*: $p<0.05$; **: $p<0.01$.

Loss of LTD in SPNs *from Gnal*$^{+/-}$ rats

Plasticity at corticostriatal synapses is widely assumed to underlie motor learning and memory, and is critically dependent on dopamine receptor-mediated transmission (Pisani *et al.*, 2005). In light of the motor deficits observed in *Gnal*$^{+/-}$ rats, SPNs membrane and synaptic properties were analyzed from WT (N=14) and *Gnal*$^{+/-}$ (N=33) rats. Recorded neurons, identified by biocytin and DARPP-32 labelling (Fig. 5A), did not display firing activity at rest and showed similar intrinsic membrane properties (Fig. 5B,C; $p>0.05$). We then examined the synaptic properties of *Gnal*$^{+/+}$ and *Gnal*$^{+/-}$ SPNs. EPSCs were evoked by synaptic stimulation of corticostriatal glutamatergic fibers with a bipolar electrode placed in the corpus callosum. Tau measurement indicated the absence of significant difference between *Gnal*$^{+/+}$ and *Gnal*$^{+/-}$ EPSC kinetics (Fig. 5D; $p>0.05$). To investigate the relative abundance of postsynaptic glutamate AMPA and NMDA receptors, AMPA/NMDA current ratios were evaluated (Fig. 5D; p=0.9779). We then analyzed short-term plasticity, by measuring the paired-pulse ratio (PPR). At short ISI (50-150 ms) of paired synaptic stimulation, a similar facilitation of synaptic transmission (PPF) was induced in both genotypes, whereas at longer ISI (200–500 ms), PPF was observed neither in *Gnal*$^{+/+}$ nor in *Gnal*$^{+/-}$ rats (Fig. 5E). Two-way ANOVA indicated a significant effect of ISI (p<0.0001) but not of genotype (p=0.2405).

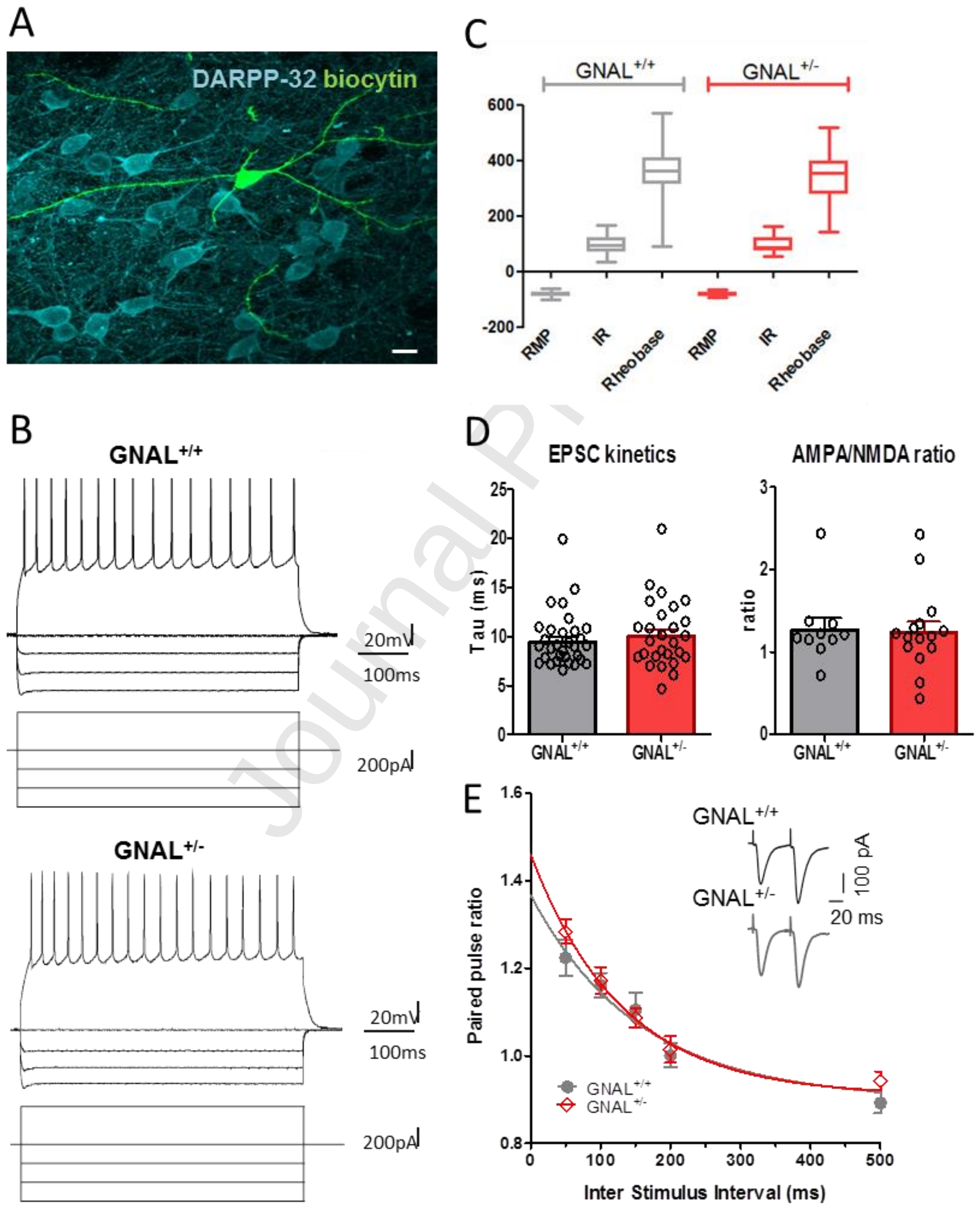

Figure 5. Intrinsic membrane and synaptic properties of striatal spiny projection neurons (SPNs) in *Gnal*$^{+/+}$ and *Gnal*$^{+/-}$ rats. (A) Confocal imaging of SPNs from a *Gnal*$^{+/-}$ slice, immunolabelled for DARPP-32 (cyano), marker of SPNs. The recorded SPN is filled

with biocytin (green) (scale bar: 50 μm). (B) Representative traces showing voltage responses of *Gnal*$^{+/+}$ and *Gnal*$^{+/-}$ SPNs to current steps in both depolarizing and hyperpolarizing direction. (C) Summary plot of basic electrophysiological properties of SPNs from *Gnal*$^{+/+}$ and *Gnal*$^{+/-}$ rats, showing no significant difference between genotypes (RMP: *Gnal*$^{+/+}$, -81.73 ± 0.99 mV, n=67; *Gnal*$^{+/-}$, -79.99 ± 0.86 mV, n=59, *p*=0.1933; IR: *Gnal*$^{+/+}$, 97.59 ± 3.56 MΩ, n=66; *Gnal*$^{+/-}$, 94.14 ± 3.24 MΩ, n=59, *p*=0.4793; rheobase: *Gnal*$^{+/+}$, 353.5 ± 11.53 pA, n=68; *Gnal*$^{+/-}$, 331.2 ± 12.15 pA, n=45; *p*=0.1983). (D) Summary plots of Tau values (left) and AMPA/NMDA ratio (right), measured from *Gnal*$^{+/+}$ and *Gnal*$^{+/-}$ EPSCs showing no significant difference between genotypes (Tau: *Gnal*$^{+/+}$, 9.47 ± 0.50 ms, n=31; *Gnal*$^{+/-}$, 10.05 ± 0.66 ms, n=27; *p*=0.4832; AMPA/NMDA ratio: *Gnal*$^{+/+}$, 1.27 ± 0.14, n=10; *Gnal*$^{+/-}$, 1.24 ± 0.13, n=15; *Mann Whitney* test *p*=0.9779). (E) Summary plot of PPR values showing similar facilitation in both genotypes. Each data point represents mean ± SEM (*Gnal*$^{+/+}$, n=30, 50 ms: 1.22 ± 0.04; 100 ms: 1.16 ± 0.03; 150 ms: 1.11 ± 0.40; *Gnal*$^{+/-}$, n=25, 50 ms: 1.28 ± 0.03; 100 ms: 1.17 ± 0.03; 150 ms: 1.09 ± 0.02; two-way ANOVA and *Bonferroni* posttest: ISI *p*<0.0001, genotype *p*=0.2405).

We then examined whether $G\alpha_{olf}$ haploinsufficiency affects long-term depression (LTD) at corticostriatal synapses. High-frequency stimulation (HFS) of corticostriatal glutamatergic afferents elicited a robust LTD in SPNs recorded from *Gnal*$^{+/+}$ rats (N=8)**.** However, in SPNs recorded from *Gnal*$^{+/-}$ rats (N=15), HFS failed to evoke any synaptic depression (Fig. 6A). No difference emerged between enkephalin (ENK)-positive and ENK-negative SPNs, representing direct- and indirect-pathway SPNs, as neither exhibited LTD, excluding potential pathway segregation (data not shown). A further set of recordings was performed from corticostriatal slices of *Gnal*$^{+/-}$ rats (N=13), in attempt to rescue LTD. After preincubation with either dopaminergic D1 or D2R agonists alone, SKF38393 and quinpirole (both 10 μM, 15-20 min), respectively, LTD could not be elicited (data not shown). Conversely, in the presence of a combination of both D1- and D2R agonists, a partial rescue of LTD was observed (Fig. 6B). Adenosine 2A (A2A) receptors are selectively expressed by D2R-SPNs, and, like D1Rs, also couple to *GNAL*/Gα(olf) and cAMP production, counteracting D2R action. We therefore pretreated *Gnal*$^{+/-}$ slices with the selective A2AR antagonist SCH442416 (20 nM, 20-30 min; N= 15 rats). Interestingly, in this experimental condition, we were able to observe a full recovery of LTD (Fig. 6C). These data suggest that GNAL mutation affects A2A receptor function, and that by relieving its inhibitory action on D2Rs, we could rescue a physiological synaptic depression**.**

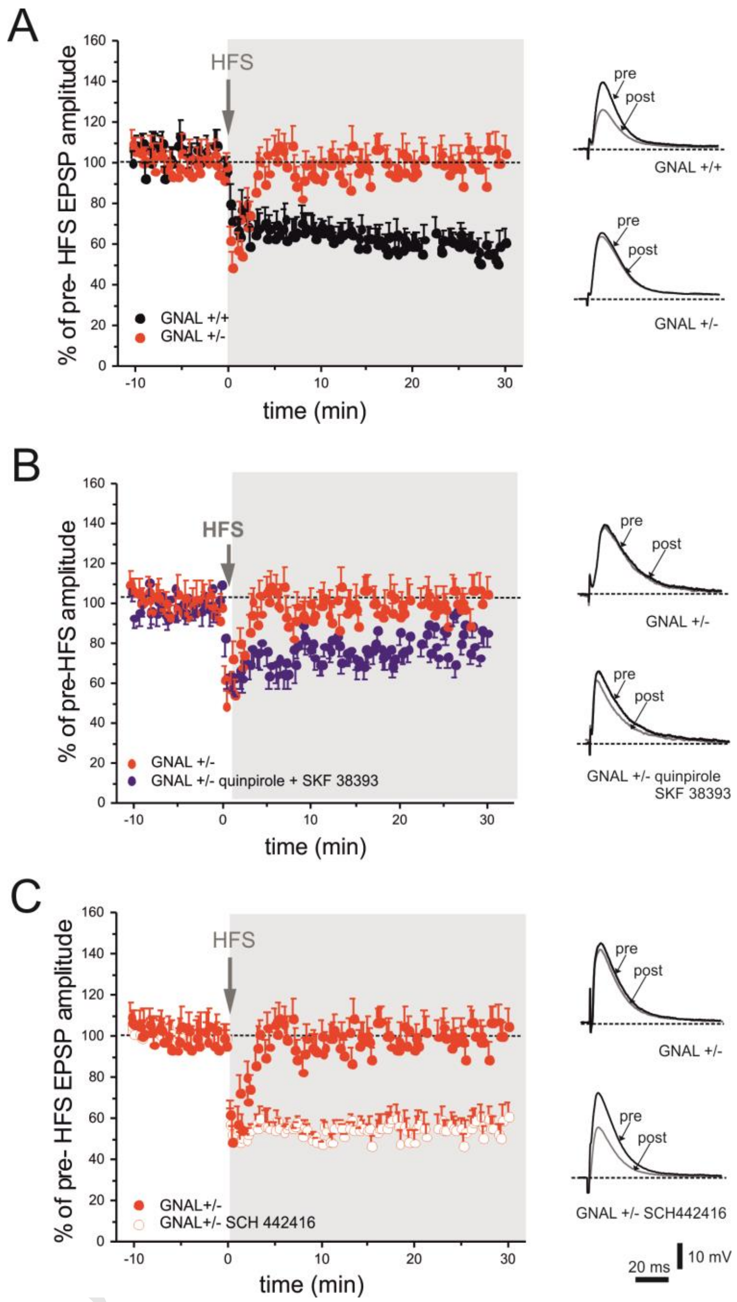

Figure 6. Impaired corticostriatal LTD in *Gnal*$^{+/-}$ rats. (A) Time-course of long-term depression (LTD) in *Gnal*$^{+/+}$ and *Gnal*$^{+/-}$ rats. High-frequency stimulation (HFS) of corticostriatal glutamatergic afferents elicit a robust LTD in SPNs recorded from *Gnal*$^{+/+}$ rats (black dots) (58.3 ± 8.3 % of control; n=18, p<0.05 Student's *t*-test), but not in SPNs from *Gnal*$^{+/-}$ rats (red dots) (106.5 ± 8.2 %, n=40, p>0.05, Student's *t*-test). Right. Sample EPSP traces are shown, measured before (pre) and 20-25 min after HFS (post). (B) Slice preincubation with a combination of dopamine D1 and D2R agonists SKF 38393 (blue dots) (10 µM) and quinpirole (10 µM) partially restores LTD (76.2 ± 7.7% of control, n = 12; Student's *t*-test p<0.05), as compared to untreated *Gnal*$^{+/-}$ SPNs (red dots). Representative traces, measured before (pre) and 20-25 min after HFS (post). (C). Pretreatment with the A2A receptor antagonist SCH 442416 (20 nM) (open dots) is able to restore a normal LTD in *Gnal*$^{+/-}$ rats (56.3 ± 4.2%, n=29, p<0.05, Mann-Whitney test), as compared to untreated

slices from *Gnal*$^{+/-}$ animals (red dots). Sample EPSPs recorded before (pre) and after (post) HFS. Data were obtained as percentage of pre-HFS EPSP amplitude for each recorded cell; each point represents mean ± SEM.

Decreased protein and mRNA expression levels of *Arc* in *Gnal*$^{+/-}$ rats

G-protein-mediated dopamine signaling phosphorylates cAMP-dependent protein kinase (PKA) via the activation of adenylyl cyclase (AC). Ultimately, CREB-dependent transcription is enhanced by the regulation of phosphorylated extracellular-signal regulated kinase (ERK) (reviewed in Nishi, Kuroiwa and Shuto, 2011). To investigate the neuropathological and molecular changes that led to decreased LTD in *Gnal*$^{+/-}$ rats", we analyzed the protein expression level of activity-regulated cytoskeleton-associated protein (ARC/ARG3.1), a CREB-target (Guzowski, 2002), which affects LTD by regulating AMPA receptor trafficking at the post-synaptic membrane (Malinow and Malenka, 2002; Chowdhury, Jason D Shepherd, *et al.*, 2006; Shepherd *et al.*, 2006; Derkach *et al.*, 2007). Western blot analysis using anti-ARC detected a distinct band at the size of approximately 45 kDa in the immunoblot. Protein expression levels of *Arc* were compared between *Gnal*$^{+/-}$ rats and WT littermates at 3 and 12 months of age (n=6 for each genotype each time point) by quantifying the intensity of the bands. Compared to WT littermates, *Gnal*$^{+/-}$ rats showed a reduction of protein expression of *Arc* by about 30% at the age of 3 months (Student's *t*-test, $p<0.01$) (Fig. 7A). However, this reduction decreased significantly at the age of 12 months and did not reach statistical significance (Student's *t*-test, $p>0.05$). Since the protein expression might differ from gene expression, we evaluated the gene expression level of *Arc* using a second cohort of rats at 12 months of age (n=8). By real-time PCR we demonstrated a significantly decreased mRNA level of *Arc* in *Gnal*$^{+/-}$ rats at this age (Student's *t*-test, $p<0.05$) (Fig. 7B).

We also determined the levels of ERK phosphorylation, which directly activates transcription factors and further enhances expression of genes including *Arc*. The phosphorylation rates of ERK1 (pERK1/ERK1) and ERK2 (pERK2/ERK2) were determined in *Gnal+/-* rats and WT littermates at 3 months of age.(n=6). There was a trend towards decreased phosphorylation rates in ERK1 (Student's t-test, p=0.0830) and ERK2 (Student's t-test, p=0.0529) (Fig. 7C and 7D).

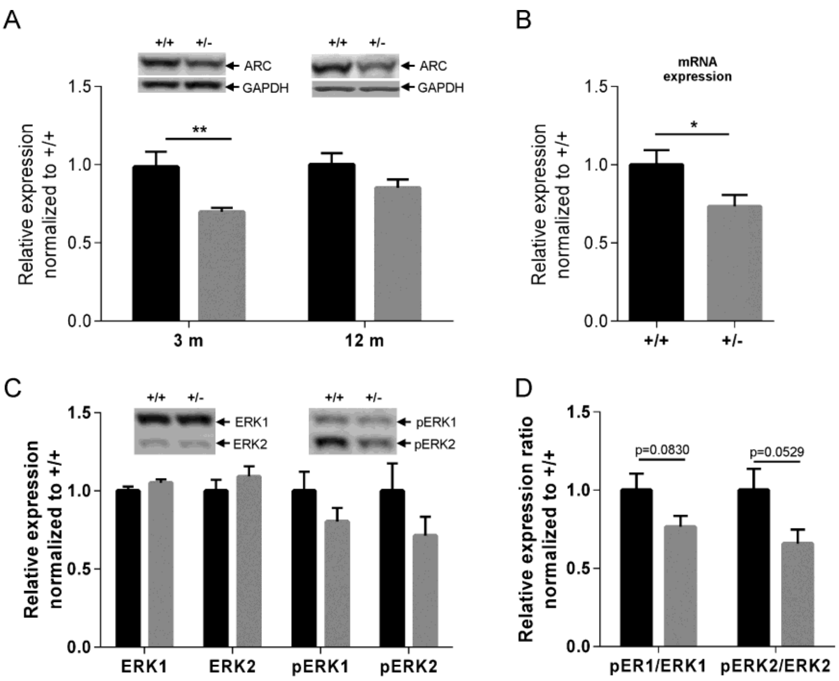

Figure 7. Reduced *Arc* expression in the striatum on the protein and mRNA levels in *Gnal*$^{+/-}$ rats. (A) Western blot analysis of ARC expression levels. Striatal brain lysates of *Gnal*$^{+/-}$ rats and WT littermates at 3 and 12 months of age 3 were immunoblotted with anti-ARC, expression of GAPDH was used as loading control (n=6 per group per age, Student's *t*-test). (B) Quantitative real-time PCR analysis of gene expression of *Arc*. mRNA was obtained from striatal tissue of 12-month-old *Gnal*$^{+/-}$ rats and WT littermates, mRNA expression of *Arc* was normalized to the geometric mean of two housekeeping genes: *Gapdh* and *Eif4a2* (n=8 per group, Student's *t*-test). (C) Western blot analysis of total expression and phosphorylation of ERK1 and ERK2 in the striatum at 3 months of age (n=6, Student's t-test). (D) Phosphorylation rates of ERK1 and ERK2 in *Gnal*+/- rats and WT littermates calculated according to the results presented in C. Student's t-test was used for statistical analysis. Data are represented as mean ± SEM. *: p<0.05; **: p<0.01. Black: +/+, grey: +/-.

Increased surface expression of AMPAR in primary striatal cells derived from *Gnal*$^{+/-}$ rats

Since a decreased *Arc* expression and reduced LTD were observed in *Gnal*$^{+/-}$ rats, we looked at whether the surface expression of AMPAR in *Gnal*$^{+/-}$ neurons was altered. Using immunofluorescence staining, we compared the average fluorescence intensity of surface AMPAR between *Gnal*$^{+/+}$ and *Gnal*$^{+/-}$ neurons. A significant increase in surface AMPAR was found in primary striatal cells derived from *Gnal*$^{+/-}$ rats compared to those derived from WT littermates, when cells were treated with a D1R agonist (SKF83822 at a dosage of 0.1µM, n=30, Student's *t*-test, *p*<0,001). However, we found no difference at basal condition (n=30, Student's *t*-test, *p*>0.05)

(Fig. 8A and 8B). These results were validated by cell surface protein biotinylation and Western blot analysis. We found a comparable expression level of AMPAR between *Gnal*$^{+/-}$ and WT neurons in all total protein fractions and the biotinylated membrane fraction at basal condition, but an increased level in the membrane fraction of *Gnal*$^{+/-}$ neurons compared to WT neurons in the SKF83822-treated group (Fig. 8C).

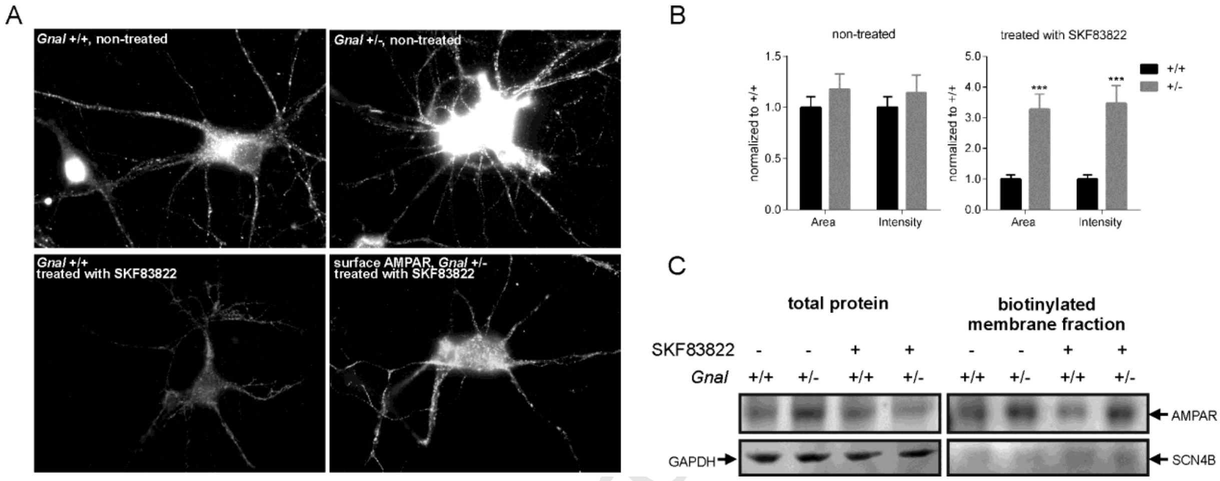

Figure 8. Increased surface expression of AMPAR in *Gnal*$^{+/-}$ striatal neurons under treatment with D1R agonist. (A) Representative images of cell surface AMPAR staining of striatal neurons. Striatal primary neurons derived from *Gnal*$^{+/-}$ and *Gnal*$^{+/+}$ embryos (E18) were fixed at DIV21 and stained with anti-AMPAR. One group of cells was treated with D1 receptor agonist 0.1 µM SKF83822 for 20 min at room temperature (RT), the non-treated group was kept for the same incubation time at RT as treated cells. Quantitative analysis showed a highly significant increase in both the area and the intensity of AMPAR-positive signals in *Gnal*$^{+/-}$ neurons compared to *Gnal*$^{+/+}$ neurons, when cells were treated with SKF83822 but not at basal condition (B) (n=30 per group, Student's *t*-test). (C) Analysis of cell surface AMPAR expression using the cell surface protein isolation kit at DIV21 showed increased AMPAR levels in the surface fraction of SKF83822-treated *Gnal*$^{+/-}$ neurons, but not in the whole cell fraction. Data are represented as mean ± SEM. ***: $p<0.001$.

Discussion

In this study, we have established a novel rat model for DTY25 by knocking out isoform 2 (UniProt G3V8E8) of the *Gnal* gene, which corresponds to the main isoform of human *GNAL* (NM_001142339.2). *Gnal*$^{+/-}$ rats showed an early-onset behavioral phenotype, as well as neurochemical and neurophysiological changes, which are associated with abnormal dopamine transmission (reviewed in Bibb, 2005; Beaulieu and Gainetdinov, 2011).

Selective ablation of Gnal isoform 2 is sufficient to cause impairment of dopamine signaling in Gnal$^{+/-}$ rats

In humans, *GNAL* isoform 2 has a higher expression level than isoform 1 (NM_182978), with a ratio of mRNA expression of approximately 10x in the striatum (Vemula *et al.*, 2013a). Similarly, we detected an 8-fold higher RNA expression level of isoform 2 compared to isoform 1 (NM 001191836) in the striatum of WT rats (data not shown). This could explain why knock-out of *Gnal* isoform 2 is sufficient to cause characteristic disease phenotypes. The *Gnal* knockout mice were generated by replacing the 1.65 kb region of *Gnal* gene, which contains the first 4 exons, with a 1.7 kb *pgk-neo* cassette, leading to a null mutation in the $G\alpha_{olf}$ protein. Most homozygous mutant mice with a complete knockout of *Gnal* failed to thrive; only very few could survive (Belluscio *et al.*, 1998). On the other hand, isoform 2 selective knock-out *Gnal*$^{-/-}$ rats showed a survival rate of about 75%, which may be due to the intact expression of *Gnal* isoform 1. Furthermore, *Gnal*$^{+/-}$ mice exhibited an impaired response to dopamine and dopamine receptor type 1 agonists, but they showed no phenotype in the non-stimulated basal state (Belluscio *et al.*, 1998; Corvol *et al.*, 2001, 2007; Pelosi *et al.*, 2017). Overall, compared to *Gnal* knockout mice, *Gnal* rats with selective ablation of isoform 2 may be a more suitable animal model for preclinical studies in DYT25, and for understanding disease mechanisms and function of the $G\alpha_{olf}$ protein.

Haploinsufficiency of *Gnal* isoform 2 may cause impaired LTD in *Gnal*$^{+/-}$ knockout rats via impaired surface expression of AMPAR mediated by reduced *Arc* expression

It is well known that activation of the AC/cAMP/PAK pathway following $G\alpha_{olf}$ coupling to D1R and A2A receptors enhances gene expression in the striatum (Kull, Svenningsson and Fredholm, 2000). ARC is one of these target proteins that regulate the cell surface expression of AMPAR by controlling the endocytic process. Accordingly, in *Arc* knockout animals, hippocampal long-term depression was significantly altered (Plath *et al.*, 2006). In this study we found reduced *Arc* expression and increased cell surface expression of AMPAR along with the loss of corticostriatal LTD in *Gnal*$^{+/-}$ rats. Although we are not aware of the mechanistic basis for such change, it is likely that *Gnal* ablation is responsible for the impairment of

$G\alpha_{olf}$ coupling to D1R, but most importantly for LTD induction, to A2A receptors (Fig. 9).

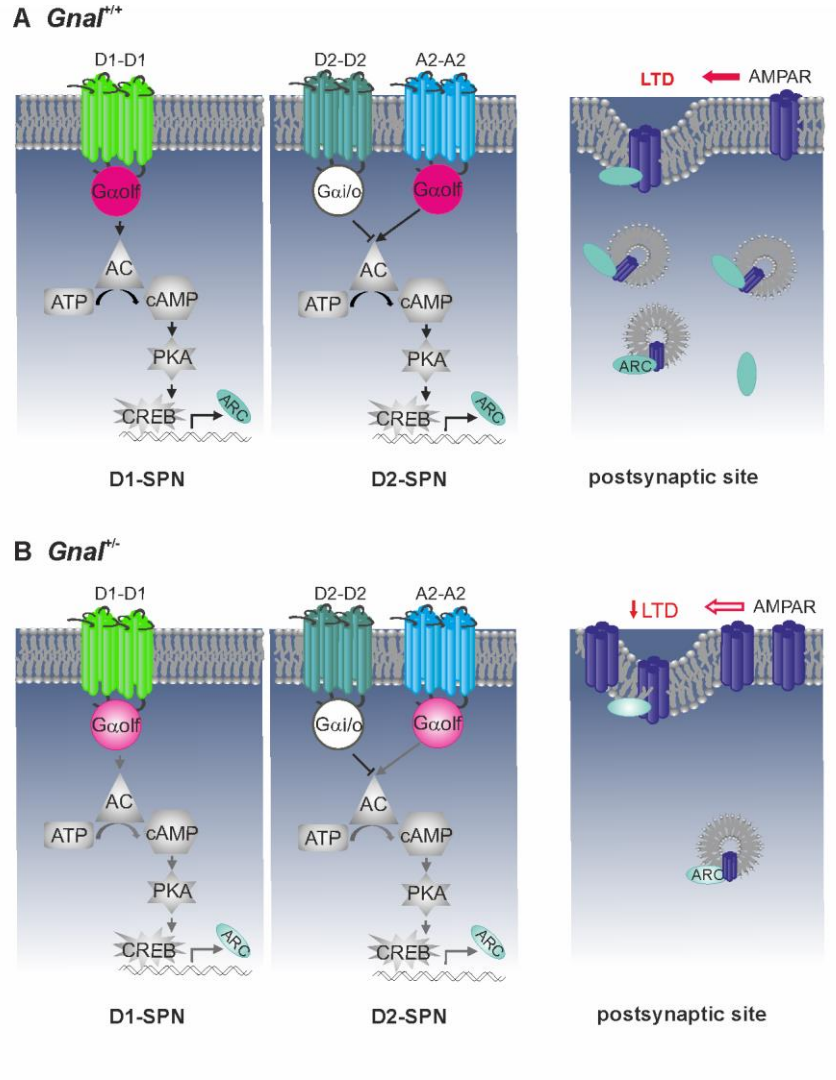

Figure 9. Schematic representation of $G\alpha_{olf}$-mediated biological processes. (A) In D1-type *Gnal*$^{+/+}$ spiny projection neurons (SPNs), the protein $G\alpha_{olf}$ couples with dimerized D1R leading to the activation of the AC-cAMP-PKA cascade and thus increases the gene expression of *Arc*, while $G\alpha_{olf}$ coupling to A2AR in D2-type SPNs counteracts D2R inhibition of AC-cAMP-PKA cascade resulting in the same effect as enhanced gene expression. At the postsynaptic sites, ARC down-regulates the cell surface expression of AMPAR by facilitating the endocytosis process, and subsequently enhancing LTD. (B) In both D1- and D2-type *Gnal*$^{+/-}$ SPNs, haploinsufficiency of $G\alpha_{olf}$ results in reduced expression of genes including *Arc*. The recycling and degradation of AMPAR mediated by endocytosis is suppressed by the lack of the Arc protein. As a result, increased synaptic expression of AMPAR prevents LTD formation, leading to decreased LTD.

We observed a reduced expression of *Arc* at both mRNA and protein levels in *Gnal+/-* rats, as well as a tendency to decreased ERK phosphorylation. Gene expression and post transcriptional regulation of *Arc* is controlled by several receptor signaling pathways including NMDA- (Steward and Worley, 2001; Bloomer, VanDongen and VanDongen, 2008), brain-derived neurotrophic factor- (Ying *et al.*, 2002), insulin- (Kremerskothen *et al.*, 2002), serotonin (Pei *et al.*, 2000)- Adreno- (McIntyre *et al.*, 2005) and dopamine and adenosine signaling pathways (Fosnaugh *et al.*, 1995; Kull et al., 2000).

Our data suggest that in *Gnal* isoform 2 selective knockout rats, haploinsufficiency of $G\alpha_{olf}$ interferes with D1R and A2A receptor signal transduction and also alters gene expression and posttranscriptional modification of *Arc*, leading to decreased protein levels. ARC associates with components of the cytoskeleton including F-actin (Lyford *et al.*, 1995), microtubules, and microtubule-associated protein 2 (MAP2) (Fujimoto *et al.*, 2004). Moreover, ARC is located at the post synaptic density (PSD), associating with the N-Methyl-D-aspartate (NMDA) receptor (Husi *et al.*, 2000; Donai *et al.*, 2003; Fujimoto *et al.*, 2004), and therefore affects glutamate transmission. At the synaptic site, ARC interacts with an inactive form of calcium/calmodulin-dependent protein kinase IIβ (CaMKIIβ), which subsequently modulates AMPA receptor trafficking. It has been reported that knock down of *Arc* or expression of mutant *Arc*, which was unable to interact with the endocytic machinery, induces density and morphology changes of spines in hippocampal neurons (Shepherd *et al.*, 2006; Waung *et al.*, 2008; Peebles *et al.*, 2010; Balu and Coyle, 2014). Interestingly, reduced spine length has been observed in the striatum of *Gnal*$^{+/-}$ mice with decreased autophosphorylation of CaMKIIβ (Pelosi *et al.*, 2017) . It raises the question if these events are associated with abnormal *Arc* expression level. However, neither mRNA nor protein expression level of *Arc* was investigated in *Gnal*$^{+/-}$ mice. Nevertheless, the localization of AMPAR depends on the exo-, and endocytosis (Beattie *et al.*, 2000; Lu *et al.*, 2007; Rosendale *et al.*, 2017), which are regulated by ARC via regulating actin cytoskeleton and interacting with components of the endocytic machinery (Lyford *et al.*, 1995; Chowdhury, Jason D. Shepherd, *et al.*, 2006). Importantly, the cell surface expression level of AMPAR plays a crucial role for the onset or magnitude of long-term potentiation (LTP) and LTD (reviewed in Malinow and Malenka, 2002; Bredt and Nicoll, 2003). Our study demonstrated an increased surface rate of AMPAR in striatal neurons from *Gnal*$^{+/-}$ rats. Furthermore, we found that LTD was impaired in SPNs of

2-month-old *Gnal*$^{+/-}$ rats. Overall, our results showed a reduction in AMPAR surface expression in *Gnal+/-* rats, which could be caused by decreased gene transcription of Arc and eventually lead to impaired corticostriatal synaptic plasticity.

What is the relationship between loss of corticostriatal LTD and reduced locomotor activity in *Gnal*$^{+/-}$ rats?

It is well known that locomotion rate and speed depend on dopamine signaling (Beninger, 1983; Zhou and Palmiter, 1995). As expected, *Gnal*$^{+/-}$ rats displayed a decreased locomotor activity over the entire study period. Corticostriatal synaptic plasticity is considered a well-established experimental paradigm of motor learning and memory, which is critically dependent on dopamine-mediated neurotransmission (Pisani et al., 2005; Surmeier et al., 2009; Lovinger 2010).

Our data showed loss of LTD and reduced ambulatory activity in *Gnal*$^{+/-}$ rats. We provide evidence showing that by inhibiting A2A receptor-mediated influence on D2Rs, we were able to restore a physiological LTD. Accordingly, it it is known that A2A receptor antagonism stimulates locomotion in mice (Kase, 2003). However, to conclude that the reduced motor activity is related to the loss of corticostriatal LTD, further evidence needs to be provided.

Motor deficits in *Gnal*$^{+/-}$ rats

The poorer rotarod performance of *Gnal*$^{+/-}$ rats compared to WT littermates indicated an impaired motor coordination. The same phenotype was observed in *Gnal*$^{+/-}$ mice (Pelosi *et al.*, 2017) and other dystonia animal models detected either by rotarod test or beam walking test (reviewed in Richter and Richter, 2014). Interestingly, impaired motor coordination was also found in mice lacking G protein γ7-subunit and type 5 adenylyl cyclase, which are important components in the D1 and A2A receptor signaling pathway such as $G\alpha_{olf}$ (Schwindinger *et al.*, 2003; Iwamoto *et al.*, 2004; Xie *et al.*, 2015). With all this evidence, we can assume that motor dysfunction detected by these tests is a disease phenotype in genetic dystonia rodents, and therefore can be used as readout and disease progression marker for therapeutic studies. Furthermore, the deficit in motor learning frequently observed in other dystonia animal models (Sharma *et al.*, 2005; Grundmann *et al.*, 2012; Pelosi *et al.*, 2017; Yu-

Taeger *et al.*, 2018) as well as in human patients (Ghilardi *et al.*, 2003) was also found in *Gnal*$^{+/-}$ rats with the rotarod test.

Homozygous *Gnal* knockout rats, which are expected to have a stronger disease phenotype, showed a high survival rate of approximately 75% compared to *Gnal* knockout mice, which may be due to expression of other isoforms of *Gnal* in our rat model. Future comparative studies between homo-, heterozygous and WT rats will provide a better understanding of $G\alpha_{olf}$ function/loss-of-function.

Conclusion

In this study we present a rat knockout model of the *Gnal* isoform 2 for DYT25. *Gnal*$^{+/-}$ rats showed early-onset phenotypes, which are associated with impaired dopamine signaling. Alterations of striatal dopamine transmission are involved in various types of dystonia (reviewed in Richter and Richter, 2014b), making the rat knockout model of *Gnal* isoform 2 a valuable tool for therapy studies, not only for DYT25, but potentially also for other types of dystonia. Notably, we have shown that impaired synaptic plasticity (LTD) is associated with increased cell surface expression of AMPAR, which might be determined by reduced expression of *Arc* in a dystonia animal model.

Acknowledgments

This work was funded by Foundation for Dystonia Research. It was also partially supported by Bundesministerium für Bildung und Forschung (BMBF) grant No. 031A575B, and FDR collaborative research projects grant No.2013-2015. We would like to thank Ms. Tina Roenisch, Ms. Larissa Lotzer, and Mr. Massimo Tolu for technical assistance. We also thank Dr. Benedikt Fabry for help with tissue preparation.

Financial and competing interests disclosure

The authors report no conflicts of interest.

REFERENCES

Albanese, A. *et al.* (2013) ‘Phenomenology and classification of dystonia: A consensus update’, *Movement Disorders*, 28(7), pp. 863–873. doi: 10.1002/mds.25475.

Andersen, C. L., Jensen, J. L. and Ørntoft, T. F. (2004) ‘Normalization of Real-Time Quantitative Reverse Transcription-PCR Data: A Model-Based Variance Estimation Approach to Identify Genes Suited for Normalization, Applied to Bladder and Colon Cancer Data Sets’, *Cancer Research*, 64(15), pp. 5245–5250. doi: 10.1158/0008-5472.CAN-04-0496.

Bagetta, V. *et al.* (2011) ‘Dopamine-Dependent Long-Term Depression Is Expressed in Striatal Spiny Neurons of Both Direct and Indirect Pathways: Implications for Parkinson’s Disease’, *Journal of Neuroscience*, 31(35), pp. 12513–12522. doi: 10.1523/JNEUROSCI.2236-11.2011.

Balu, D. T. and Coyle, J. T. (2014) ‘Chronic D-serine reverses arc expression and partially rescues dendritic abnormalities in a mouse model of NMDA receptor hypofunction’, *Neurochemistry International*, 75, pp. 76–78. doi: 10.1016/j.neuint.2014.05.015.

Barry, M. F. and Ziff, E. B. (2002) ‘Receptor trafficking and the plasticity of excitatory synapses.’, *Current opinion in neurobiology*, 12(3), pp. 279–86. Available at: http://www.ncbi.nlm.nih.gov/pubmed/12049934.

Beattie, E. C. *et al.* (2000) ‘Regulation of AMPA receptor endocytosis by a signaling mechanism shared with LTD’, *Nature Neuroscience*, 3(12), pp. 1291–1300. doi: 10.1038/81823.

Beaulieu, J.-M. and Gainetdinov, R. R. (2011) ‘The physiology, signaling, and pharmacology of dopamine receptors.’, *Pharmacological reviews*, 63(1), pp. 182–217. doi: 10.1124/pr.110.002642.

Belluscio, L. *et al.* (1998) ‘Mice deficient in G(olf) are anosmic.’, *Neuron*, 20(1), pp. 69–81. Available at: http://www.ncbi.nlm.nih.gov/pubmed/9459443.

Beninger, R. J. (1983) ‘The role of dopamine in locomotor activity and learning.’, *Brain research*, 287(2), pp. 173–96. Available at: http://www.ncbi.nlm.nih.gov/pubmed/6357357.

Berke, J. D. *et al.* (1998) ‘A complex program of striatal gene expression induced by dopaminergic stimulation.’, *The Journal of neuroscience : the official journal of the Society for Neuroscience*, 18(14), pp. 5301–10. Available at: http://www.ncbi.nlm.nih.gov/pubmed/9651213.

Bibb, J. A. (2005) ‘Decoding dopamine signaling.’, *Cell*, 122(2), pp. 153–5. doi: 10.1016/j.cell.2005.07.011.

Bloomer, W. A. C., VanDongen, H. M. A. and VanDongen, A. M. J. (2008) ‘Arc/Arg3.1 translation is controlled by convergent N-methyl-D-aspartate and Gs-coupled receptor signaling pathways.’, *The Journal of biological chemistry*, 283(1), pp. 582–92. doi: 10.1074/jbc.M702451200.

Bredt, D. S. and Nicoll, R. A. (2003) ‘AMPA receptor trafficking at excitatory synapses.’, *Neuron*, 40(2), pp. 361–79. Available at: http://www.ncbi.nlm.nih.gov/pubmed/14556714.

Chowdhury, S., Shepherd, J. D., *et al.* (2006) ‘Arc/Arg3.1 interacts with the endocytic machinery to regulate AMPA receptor trafficking.’, *Neuron*, 52(3), pp. 445–59. doi: 10.1016/j.neuron.2006.08.033.

Chowdhury, S., Shepherd, J. D., *et al.* (2006) ‘Arc/Arg3.1 Interacts with the Endocytic Machinery to Regulate AMPA Receptor Trafficking’, *Neuron*, 52(3), pp. 445–459. doi: 10.1016/j.neuron.2006.08.033.

Cole, A. J. *et al.* (1992) ‘D1 dopamine receptor activation of multiple transcription factor genes in rat striatum.’, *Journal of neurochemistry*, 58(4), pp. 1420–6. Available at: http://www.ncbi.nlm.nih.gov/pubmed/1347779.

Cong, L. *et al.* (2013) ‘Multiplex Genome Engineering Using CRISPR/Cas Systems’, *Science*, 339(6121), pp. 819–823. doi: 10.1126/science.1231143.

Cortall, B. and Naylor, R. J. (1997) ‘Behavioural aspects of dopamine agonists and antagonists’, in Horn, A. S., Korf, J., and Westerink, B. H. C. (eds) *The Neurobiology of Dopamine*. The neurob. London: Academic Press, pp. 555–576.

Corvol, J.-C. *et al.* (2007) ‘Quantitative changes in Galphaolf protein levels, but not D1 receptor, alter specifically acute responses to psychostimulants.’, *Neuropsychopharmacology : official publication of the American College of Neuropsychopharmacology*, 32(5), pp. 1109–21. doi: 10.1038/sj.npp.1301230.

Corvol, J. C. *et al.* (2001) ‘Galpha(olf) is necessary for coupling D1 and A2a receptors to adenylyl cyclase in the striatum.’, *Journal of neurochemistry*, 76(5), pp. 1585–8. Available at: http://www.ncbi.nlm.nih.gov/pubmed/11238742.

Cui, G. *et al.* (2013) ‘Concurrent activation of striatal direct and indirect pathways during action initiation.’, *Nature*, 494(7436), pp. 238–42. doi: 10.1038/nature11846.

Derkach, V. A. *et al.* (2007) ‘Regulatory mechanisms of AMPA receptors in synaptic plasticity.’, *Nature reviews. Neuroscience*, 8(2), pp. 101–13. doi: 10.1038/nrn2055.

Donai, H. *et al.* (2003) ‘Interaction of Arc with CaM kinase II and stimulation of neurite extension by Arc in neuroblastoma cells expressing CaM kinase II.’, *Neuroscience research*, 47(4), pp. 399–408. Available at: http://www.ncbi.nlm.nih.gov/pubmed/14630344.

Drinnan, S. L. *et al.* (1991) ‘G(olf) in the basal ganglia.’, *Molecular and cellular neurosciences*, 2(1), pp. 66–70. Available at: http://www.ncbi.nlm.nih.gov/pubmed/19912784.

Fosnaugh, J. S. *et al.* (1995) ‘Activation of arc, a putative "effector" immediate early gene, by cocaine in rat brain.’, *Journal of neurochemistry*, 64(5), pp. 2377–80. Available at: http://www.ncbi.nlm.nih.gov/pubmed/7722525.

Friedman, W. J. *et al.* (1993) ‘Differential actions of neurotrophins in the locus coeruleus and basal forebrain.’, *Experimental neurology*, 119(1), pp. 72–8. doi: 10.1006/exnr.1993.1007.

Fuchs, T. *et al.* (2013) ‘Mutations in GNAL cause primary torsion dystonia.’, *Nature genetics*, 45(1), pp. 88–92. doi: 10.1038/ng.2496.

Fujimoto, T. *et al.* (2004) ‘Arc interacts with microtubules/microtubule-associated protein 2 and attenuates microtubule-associated protein 2 immunoreactivity in the dendrites’, *Journal of Neuroscience Research*, 76(1), pp. 51–63. doi: 10.1002/jnr.20056.

Gerfen, C. R. and Surmeier, D. J. (2011) ‘Modulation of striatal projection systems by dopamine.’, *Annual review of neuroscience*. NIH Public Access, 34, pp. 441–66. doi: 10.1146/annurev-neuro-061010-113641.

Ghilardi, M.-F. *et al.* (2003) ‘Impaired sequence learning in carriers of the DYT1 dystonia mutation.’, *Annals of neurology*, 54(1), pp. 102–9. doi: 10.1002/ana.10610.

Giordano, N. *et al.* (2018) ‘Motor learning and metaplasticity in striatal neurons: relevance for Parkinson’s disease’, *Brain*. Oxford University Press, 141(2), pp. 505–520. doi: 10.1093/brain/awx351.

Goodchild, R. E., Grundmann, K. and Pisani, A. (2013) ‘New genetic insights highlight “old” ideas on motor dysfunction in dystonia’, *Trends in Neurosciences*, 36(12), pp. 717–725. doi: 10.1016/j.tins.2013.09.003.

Grundmann, K. *et al.* (2012) ‘Generation of a novel rodent model for DYT1 dystonia’, *Neurobiology of Disease*, 47(1), pp. 61–74. doi: 10.1016/j.nbd.2012.03.024.

Guzowski, J. F. (2002) ‘Insights into immediate-early gene function in hippocampal memory consolidation using antisense oligonucleotide and fluorescent imaging approaches.’, *Hippocampus*, 12(1), pp. 86–104. doi: 10.1002/hipo.10010.

Harms, D. W. *et al.* (2014) ‘Mouse Genome Editing Using the CRISPR/Cas System’, in *Current Protocols in Human Genetics*. Hoboken, NJ, USA: John Wiley & Sons, Inc., p. 15.7.1-15.7.27. doi: 10.1002/0471142905.hg1507s83.

Hervé, D. *et al.* (1993) ‘G(olf) and Gs in rat basal ganglia: possible involvement of G(olf) in the coupling of dopamine D1 receptor with adenylyl cyclase.’, *The Journal of neuroscience : the official journal of the Society for Neuroscience*, 13(5), pp. 2237–48. Available at: http://www.ncbi.nlm.nih.gov/pubmed/8478697.

Hervé, D. *et al.* (2001) ‘Galpha(olf) levels are regulated by receptor usage and control dopamine and adenosine action in the striatum.’, *The Journal of neuroscience : the official journal of the Society for Neuroscience*, 21(12), pp. 4390–9. Available at: http://www.ncbi.nlm.nih.gov/pubmed/11404425.

Hervé, D., Rogard, M. and Lévi-Strauss, M. (1995) ‘Molecular analysis of the multiple Golf alpha subunit mRNAs in the rat brain.’, *Brain research. Molecular brain research*, 32(1), pp. 125–34. Available at: http://www.ncbi.nlm.nih.gov/pubmed/7494450.

Husi, H. *et al.* (2000) ‘Proteomic analysis of NMDA receptor–adhesion protein signaling complexes’, *Nature Neuroscience*, 3(7), pp. 661–669. doi: 10.1038/76615.

Iwamoto, T. *et al.* (2004) ‘Disruption of type 5 adenylyl cyclase negates the developmental increase in Galphaolf expression in the striatum.’, *FEBS letters*, 564(1–2), pp. 153–6. doi: 10.1016/S0014-5793(04)00333-3.

Jayanthi, S. *et al.* (2009) 'Methamphetamine induces dopamine D1 receptor-dependent endoplasmic reticulum stress-related molecular events in the rat striatum.', *PloS one*. Edited by B. T. Baune, 4(6), p. e6092. doi: 10.1371/journal.pone.0006092.

Jones, D. T. and Reed, R. R. (1989) 'Golf: an olfactory neuron specific-G protein involved in odorant signal transduction.', *Science (New York, N.Y.)*, 244(4906), pp. 790–5. Available at: http://www.ncbi.nlm.nih.gov/pubmed/2499043.

Kaneko, T. (2017) 'Genome Editing of Rat', in *Methods in molecular biology (Clifton, N.J.)*, pp. 101–108. doi: 10.1007/978-1-4939-7128-2_9.

Kase, H. (2003) 'Industry forum: Progress in pursuit of therapeutic A2A antagonists: The adenosine A2A receptor selective antagonist KW6002: Research and development toward a novel nondopaminergic therapy for Parkinson's disease', *Neurology*, 61(Issue 11, Supplement 6), pp. S97–S100. doi: 10.1212/01.WNL.0000095219.22086.31.

Kebabian, J. W., Petzold, G. L. and Greengard, P. (1972) 'Dopamine-sensitive adenylate cyclase in caudate nucleus of rat brain, and its similarity to the "dopamine receptor".', *Proceedings of the National Academy of Sciences of the United States of America*, 69(8), pp. 2145–9. Available at: http://www.ncbi.nlm.nih.gov/pubmed/4403305.

Klein, C. (2014) 'Genetics in dystonia', *Parkinsonism & Related Disorders*, 20, pp. S137–S142. doi: 10.1016/S1353-8020(13)70033-6.

Kremerskothen, J. *et al.* (2002) 'Insulin-induced expression of the activity-regulated cytoskeleton-associated gene (ARC) in human neuroblastoma cells requires p21(ras), mitogen-activated protein kinase/extracellular regulated kinase and src tyrosine kinases but is protein kinase C-independent.', *Neuroscience letters*, 321(3), pp. 153–6. Available at: http://www.ncbi.nlm.nih.gov/pubmed/11880195.

Kull, B., Svenningsson, P. and Fredholm, B. B. (2000) 'Adenosine A(2A) receptors are colocalized with and activate g(olf) in rat striatum.', *Molecular pharmacology*, 58(4), pp. 771–7. Available at: http://www.ncbi.nlm.nih.gov/pubmed/10999947.

Kumar, K. R. *et al.* (2014) 'Mutations in *GNAL*', *JAMA Neurology*, 71(4), p. 490. doi: 10.1001/jamaneurol.2013.4677.

Lu, J. *et al.* (2007) 'Postsynaptic positioning of endocytic zones and AMPA receptor cycling by physical coupling of dynamin-3 to Homer.', *Neuron*. NIH Public Access, 55(6), pp. 874–89. doi: 10.1016/j.neuron.2007.06.041.

Lyford, G. L. *et al.* (1995) 'Arc, a growth factor and activity-regulated gene, encodes a novel cytoskeleton-associated protein that is enriched in neuronal dendrites.', *Neuron*, 14(2), pp. 433–45. Available at: http://www.ncbi.nlm.nih.gov/pubmed/7857651.

Malinow, R. and Malenka, R. C. (2002) 'AMPA receptor trafficking and synaptic plasticity.', *Annual review of neuroscience*, 25(1), pp. 103–26. doi: 10.1146/annurev.neuro.25.112701.142758.

Maltese, M. *et al.* (2018) 'Early structural and functional plasticity alterations in a susceptibility period of DYT1 dystonia mouse striatum.', *eLife*, 7. doi:

10.7554/eLife.33331.

Masters, S. B., Stroud, R. M. and Bourne, H. R. (no date) ‘Family of G protein alpha chains: amphipathic analysis and predicted structure of functional domains.’, *Protein engineering*, 1(1), pp. 47–54. Available at: http://www.ncbi.nlm.nih.gov/pubmed/3148932.

Masuho, I. *et al.* (2016) ‘Homozygous *GNAL* mutation associated with familial childhood-onset generalized dystonia’, *Neurology Genetics*, 2(3), p. e78. doi: 10.1212/NXG.0000000000000078.

McIntyre, C. K. *et al.* (2005) ‘Memory-influencing intra-basolateral amygdala drug infusions modulate expression of Arc protein in the hippocampus.’, *Proceedings of the National Academy of Sciences of the United States of America*, 102(30), pp. 10718–23. doi: 10.1073/pnas.0504436102.

Nishi, A., Kuroiwa, M. and Shuto, T. (2011) ‘Mechanisms for the modulation of dopamine d(1) receptor signaling in striatal neurons.’, *Frontiers in neuroanatomy*. Frontiers Media SA, 5, p. 43. doi: 10.3389/fnana.2011.00043.

Oleas, J. *et al.* (2013) ‘Engineering animal models of dystonia.’, *Movement disorders : official journal of the Movement Disorder Society*, 28(7), pp. 990–1000. doi: 10.1002/mds.25583.

Packard, M. G. and Knowlton, B. J. (2002) ‘Learning and memory functions of the Basal Ganglia.’, *Annual review of neuroscience*, 25(1), pp. 563–93. doi: 10.1146/annurev.neuro.25.112701.142937.

Peebles, C. L. *et al.* (2010) ‘Arc regulates spine morphology and maintains network stability in vivo.’, *Proceedings of the National Academy of Sciences of the United States of America*, 107(42), pp. 18173–8. doi: 10.1073/pnas.1006546107.

Pei, Q. *et al.* (2000) ‘Serotonergic regulation of mRNA expression of Arc, an immediate early gene selectively localized at neuronal dendrites.’, *Neuropharmacology*, 39(3), pp. 463–70. Available at: http://www.ncbi.nlm.nih.gov/pubmed/10698012.

Pelosi, A. *et al.* (2017) ‘Heterozygous Gnal Mice Are a Novel Animal Model with Which to Study Dystonia Pathophysiology.’, *The Journal of neuroscience : the official journal of the Society for Neuroscience*, 37(26), pp. 6253–6267. doi: 10.1523/JNEUROSCI.1529-16.2017.

Pfaffl, M. W. (2001) ‘A new mathematical model for relative quantification in real-time RT-PCR.’, *Nucleic acids research*, 29(9), p. e45. Available at: http://www.ncbi.nlm.nih.gov/pubmed/11328886.

Pisani, A. *et al.* (2005) ‘Striatal synaptic plasticity: Implications for motor learning and Parkinson’s disease’, *Movement Disorders*, 20(4), pp. 395–402. doi: 10.1002/mds.20394.

Plath, N. *et al.* (2006) ‘Arc/Arg3.1 Is Essential for the Consolidation of Synaptic Plasticity and Memories’, *Neuron*, 52(3), pp. 437–444. doi: 10.1016/j.neuron.2006.08.024.

Richter, F. and Richter, A. (2014a) ‘Genetic animal models of dystonia: Common features and diversities', *Progress in Neurobiology*, 121, pp. 91–113. doi: 10.1016/j.pneurobio.2014.07.002.

Richter, F. and Richter, A. (2014b) 'Genetic animal models of dystonia: Common features and diversities', *Progress in Neurobiology*, 121, pp. 91–113. doi: 10.1016/j.pneurobio.2014.07.002.

Rosendale, M. *et al.* (2017) 'Spatial and Temporal Regulation of Receptor Endocytosis in Neuronal Dendrites Revealed by Imaging of Single Vesicle Formation', *Cell Reports*, 18. doi: 10.1016/j.celrep.2017.01.081.

Rumbaugh, G. *et al.* (2003) 'Synapse-associated protein-97 isoform-specific regulation of surface AMPA receptors and synaptic function in cultured neurons.', *The Journal of neuroscience : the official journal of the Society for Neuroscience*, 23(11), pp. 4567–76. Available at: http://www.ncbi.nlm.nih.gov/pubmed/12805297.

Schwindinger, W. F. *et al.* (2003) 'Loss of G protein gamma 7 alters behavior and reduces striatal alpha(olf) level and cAMP production.', *The Journal of biological chemistry*, 278(8), pp. 6575–9. doi: 10.1074/jbc.M211132200.

Schwindinger, W. F. *et al.* (2010) 'Adenosine A $_{2A}$ Receptor Signaling and G $_{olf}$ Assembly Show a Specific Requirement for the γ $_{7}$ Subtype in the Striatum', *Journal of Biological Chemistry*, 285(39), pp. 29787–29796. doi: 10.1074/jbc.M110.142620.

Sharma, N. *et al.* (2005) 'Impaired Motor Learning in Mice Expressing TorsinA with the DYT1 Dystonia Mutation', *Journal of Neuroscience*, 25(22), pp. 5351–5355. doi: 10.1523/JNEUROSCI.0855-05.2005.

Shepherd, J. D. *et al.* (2006) 'Arc/Arg3.1 mediates homeostatic synaptic scaling of AMPA receptors.', *Neuron*, 52(3), pp. 475–84. doi: 10.1016/j.neuron.2006.08.034.

Shiotsuki, H. *et al.* (2010) 'A rotarod test for evaluation of motor skill learning.', *Journal of neuroscience methods*, 189(2), pp. 180–5. doi: 10.1016/j.jneumeth.2010.03.026.

Steward, O. and Worley, P. F. (2001) 'Selective targeting of newly synthesized Arc mRNA to active synapses requires NMDA receptor activation.', *Neuron*, 30(1), pp. 227–40. Available at: http://www.ncbi.nlm.nih.gov/pubmed/11343657.

Ungerstedt, U. (1979) 'Central dopamine mechanisms and behaviourNo Title', in Horn.A.S, Korf, J., and Westerink, B. H. . (eds) *The Neurobiology of Dopamine*. London: Academic Press, pp. 577–596.

Vandesompele, J. *et al.* (2002) 'Accurate normalization of real-time quantitative RT-PCR data by geometric averaging of multiple internal control genes.', *Genome biology*, 3(7), p. RESEARCH0034. Available at: http://www.ncbi.nlm.nih.gov/pubmed/12184808.

Vemula, S. R. *et al.* (2013a) 'Role of Gα(olf) in familial and sporadic adult-onset primary dystonia', *Human Molecular Genetics*, 22(12), pp. 2510–2519. doi: 10.1093/hmg/ddt102.

Vemula, S. R. *et al.* (2013b) 'Role of Gα(olf) in familial and sporadic adult-onset primary dystonia', *Human Molecular Genetics*, 22(12), pp. 2510–2519. doi: 10.1093/hmg/ddt102.

Waung, M. W. *et al.* (2008) 'Rapid translation of Arc/Arg3.1 selectively mediates mGluR-dependent LTD through persistent increases in AMPAR endocytosis rate.', *Neuron*, 59(1), pp. 84–97. doi: 10.1016/j.neuron.2008.05.014.

Willuhn, I. and Steiner, H. (2009) 'Skill-memory consolidation in the striatum: critical for late but not early long-term memory and stabilized by cocaine.', *Behavioural brain research*, 199(1), pp. 103–7. doi: 10.1016/j.bbr.2008.07.010.

Xie, K. *et al.* (2015) 'Stable G protein-effector complexes in striatal neurons: mechanism of assembly and role in neurotransmitter signaling', *eLife*, 4. doi: 10.7554/eLife.10451.

Ying, S.-W. *et al.* (2002) 'Brain-derived neurotrophic factor induces long-term potentiation in intact adult hippocampus: requirement for ERK activation coupled to CREB and upregulation of Arc synthesis.', *The Journal of neuroscience : the official journal of the Society for Neuroscience*, 22(5), pp. 1532–40. Available at: http://www.ncbi.nlm.nih.gov/pubmed/11880483.

Yu-Taeger, L. *et al.* (2012) 'A novel BACHD transgenic rat exhibits characteristic neuropathological features of Huntington disease.', *The Journal of neuroscience : the official journal of the Society for Neuroscience*, 32(44), pp. 15426–38. doi: 10.1523/JNEUROSCI.1148-12.2012.

Yu-Taeger, L. *et al.* (2018) 'Dynamic nuclear envelope phenotype in rats overexpressing mutated human torsinA protein', *Biology Open*, p. bio.032839. doi: 10.1242/bio.032839.

Zhang, D. *et al.* (2002) 'The dopamine D1 receptor is a critical mediator for cocaine-induced gene expression.', *Journal of neurochemistry*, 82(6), pp. 1453–64. Available at: http://www.ncbi.nlm.nih.gov/pubmed/12354293.

Zhou, Q. Y. and Palmiter, R. D. (1995) 'Dopamine-deficient mice are severely hypoactive, adipsic, and aphagic.', *Cell*, 83(7), pp. 1197–209. Available at: http://www.ncbi.nlm.nih.gov/pubmed/8548806.

Zhuang, X., Belluscio, L. and Hen, R. (2000) 'G(olf)alpha mediates dopamine D1 receptor signaling.', *The Journal of neuroscience : the official journal of the Society for Neuroscience*, 20(16), p. RC91. Available at: http://www.ncbi.nlm.nih.gov/pubmed/10924528.

Highlights

- Selective ablation of *Gnal* isoform 2 is sufficient to cause impairment of dopamine- and adenosine- dependent signaling in $Gnal^{+/-}$ rats
- $Gnal^{+/-}$ rats showed reduced locomotion, and impaired motor function and motor learning skills
- $Gnal^{+/-}$ rats showed loss of corticostriatal LTD, increased surface expression of AMPARs along with reduced *Arc* expression
- The loss of LTD in $Gnal^{+/-}$ rats is attributable to the impairment of $G\alpha_{olf}$ coupling to A2A receptors